

## Silyl Cations in the Solid and in Solution

Joseph B. Lambert,\* Shizhong Zhang, and Sol M. Ciro

Department of Chemistry, Northwestern University, Evanston, Illinois 60208-3113

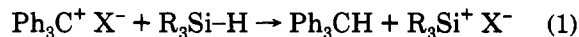
Received January 27, 1994\*

Reaction of silanes with triphenylmethyl tetrakis(pentafluorophenyl)borate (TPFPB) with excess silane as solvent yields a white solid that may be examined directly or dissolved for experiments in solution. The NMR properties of the material in a variety of solvents indicate that the anion is free and unperturbed by the presence of the silicon species. The  $^{29}\text{Si}$  chemical shift is highly dependent on the nucleophilicity of the solvent, with large downfield shifts (compared with the analogous silane,  $\Delta\delta$ ) in the order acetonitrile, sulfolane, toluene, benzene. The largest  $\Delta\delta$  values for alkyl substituents in the arene solvents are ca. 100 ppm, far short of the expectation for a fully trigonal silylium ion. For tris(trimethylsilyl)silylium tetrakis(pentafluorophenyl)borate  $\Delta\delta$  is 228.5 ppm, much closer to the trigonal ideal. The  $^{29}\text{Si}$  shifts of the solid, which had never been exposed to a solvent, are almost identical to those in benzene solution. For the case of methyldiisopropylsilane, with diastereotopic methyl groups, conversion to the TPFPB salt resulted in homotopic protons and carbons in a variety of solvents, which require a dynamic process between bound and unbound silyl species with a barrier of no more than about 13 kcal mol $^{-1}$ . The X-ray crystallographic structure of triethylsilylium tetrakis(pentafluorophenyl)borate recrystallized from hexane/toluene contains silicon in a distorted pyramid with normal coordination to the methylene carbons (1.85 Å) and an experimentally unprecedented distant coordination to toluene (2.18 Å). This Si-C distance to the para position of toluene is equivalent to a bond order of 0.28 according to the Pauling equation. The coordinated toluene is planar and essentially unaltered by the interaction with silicon, in contrast to the crystal structures of known arenium ions ( $\sigma$  complexes). The solid state  $^{13}\text{C}$  spectrum indicates little transfer of positive charge to toluene. Thus the arenium ion model is rejected by experiment. The ions are best termed silyl cations with weak  $\eta^1 \pi$  coordination to toluene.

During the last two decades, chemists have prepared a host of new structures incorporating novel functionalities with silicon in roles that are common in analogous carbon chemistry: the carbon-silicon double bond (silenes $^1$ ), the silicon-silicon double bond (disilenes $^1$ ), silaarenes, $^1$  divalent silicon (silylenes $^2$ ), and the silicon-heteroatom double bond. $^1$  The most difficult cases have proved to be the analogues to the carbonyl group $^1$  (Si=O) and to the carbenium ion ( $\text{R}_3\text{Si}^+$ ). In the latter case, which is the subject of this study, the problem is clearly not thermodynamics, as such species have long been observed in the gas phase. $^{3-5}$  In condensed phase, the high electrophilicity of the silylium ion gives rise to low kinetic stability. Strategies to observe long-lived silylium ions therefore must consider the reactivities of the solvent, the anion, and any byproducts of reagents used to generate the cation. These reactivities may in part be modulated by the steric and electronic effects of the substituents on silicon. Our experimental strategy involved evolution of each of these structural aspects.

**Cation Generation.** Loss of a leaving group in the fashion that is traditional in carbocation chemistry ( $\text{R}_3\text{C-X} \rightarrow \text{R}_3\text{C}^+ \text{X}^-$ ) is generally unsuitable in the silicon context

because of internal return involving reaction or binding of the departed anion with the silyl cation. Removal of the anion through the use of silver salts has proved feasible in the analogous tin case $^6$  but to date has not been successful with silicon. Almost all heteroatoms X have a stronger bond to silicon than they do to carbon, making them less effective leaving groups. One of the few atoms with a stronger bond to carbon than to silicon is hydrogen. Corey $^7$  and others took advantage of this difference to provide an approach to generating silyl cations based on an analogy to the Bartlett-Condon-Schneider intermolecular hydride-transfer reaction ( $\text{R}_3\text{C}^+ + \text{R}'_3\text{C-H} \rightarrow \text{R}_3\text{C-H} + \text{R}'_3\text{C}^+$ ). In the silicon analogue, a carbocation reacts with a silicon hydride to yield a silyl cation and a hydrocarbon (eq 1). Because the triphenylmethyl (trityl)



cation is readily available with a variety of anions, this reaction has proved to be practical and effective in generating species that are silyl cations, tight ion pairs, covalent species, or cations bound or complexed to solvent. $^8$  Essentially all recent studies have used this approach, since the leaving hydride has been removed entirely by covalent bonding with carbon. The byproduct triphenylmethane appears to be nonreactive. Moreover, the disappearance of the Si-H resonance and the appearance of the C-H

\* Abstract published in *Advance ACS Abstracts*, May 1, 1994.

(1) Raabe, G.; Michl, J. In *The Chemistry of Organic Silicon Compounds*; Patai, S., Rappoport, Z., Eds.; Wiley: Chichester, U.K., 1989; Part 2, pp 1015-1142.

(2) Gaspar, P. P. In *Reactive Intermediates*; Jones, M., Jr., Moss, R. A., Eds.; Wiley: New York, 1985, Vol. 3, pp 333-427.

(3) Hobrock, B. G.; Kiser, R. W. *J. Phys. Chem.* **1962**, *66*, 155-158.

(4) Weber, W. P.; Felix, R. A.; Willard, A. K. *Tetrahedron Lett.* **1970**, 907-910.

(5) Murphy, M. K.; Beauchamp, J. L. *J. Am. Chem. Soc.* **1977**, *99*, 2085-2089. Pietro, W. J.; Hehre, W. J. *J. Am. Chem. Soc.* **1982**, *104*, 4329-4332.

(6) Lambert, J. B.; Kuhlmann, B. *J. Chem. Soc., Chem. Commun.* **1992**, 931-932.

(7) Corey, J. Y. *J. Am. Chem. Soc.* **1975**, *97*, 3237-3238. Corey, J. Y.; Gust, D.; Mislow, K. *J. Organomet. Chem.* **1975**, *101*, C7-C8.

(8) Lambert, J. B.; Schulz, W. J., Jr.; McConnell, J. A.; Schilf, W. J. *Am. Chem. Soc.* **1988**, *110*, 2201-2210. Lambert, J. B.; Kania, L.; Schilf, W.; McConnell, J. A. *Organometallics* **1991**, *10*, 2578-2584.

resonance provide straightforward assays for the completion of the reaction.

**Solvent.** Generation of charged species requires a polar medium, but if the solvent is highly nucleophilic (or, more accurately, silaphilic), the silylium ion will react with it. Thus aqueous and alcoholic solvents must be avoided, and highly acidic media, which normally contain available silaphilic fluorine or chlorine atoms, are probably impractical. The presence of water would lead immediately to hydrolysis (eq 2) and the presence of other nucleophiles (N) to complex formation (eq 3). Our previous studies showed that hydrolysis had been eliminated as a factor.<sup>8</sup>



In past studies we sought evidence for silyl cations in polar solvents with low nucleophilicity, including sulfolane, dichloromethane, and 1,2-dichloroethane.<sup>8</sup> Sakurai,<sup>9</sup> Boudjouk,<sup>10</sup> and their co-workers have respectively found evidence for complexation of silylium ions with ethers and with nitriles, as in eq 3. In the present study we have turned to aromatic solvents devoid of heteroatoms.<sup>6,11</sup> Finally, we have found that it is possible to generate silyl cations directly in the solid state, without exposure to solvent other than excess silane from eq 1.

**Anion.** Widely used anions such as  $BF_4^-$  and  $SbCl_6^-$ , which have proved successful for many cations, are not practical for silyl cations, because of the silaphilic nature of the halogens. We also found that triflate and azide form covalent bonds or very tight ion pairs with silylium.<sup>8</sup> Perchlorate produced ion pairs in dichloromethane and unpaired ions complexed to solvent in acetonitrile and sulfolane.<sup>8</sup> The search for weakly coordinating anions in inorganic chemistry has a long history,<sup>12</sup> and more recent work in the context of silyl cations has moved toward arylborates<sup>6,9-11</sup> and carborane anions.<sup>13</sup> Our own work has concentrated on tetrakis(pentafluorophenyl)borate (TPFPB),<sup>6,11,14</sup> inspired by the success of Marks with cations of zirconium and thorium.<sup>15</sup> Other workers<sup>9,10,13</sup> have been examining tetrakis[bis(3,5-trifluoromethyl)phenyl]borate and *closo*-carboranes.

**Substituent.** Favorable properties of substituents include large size, high polarizability, and ability to donate electrons. Size may be critical to decrease the ability of nucleophiles to attack the silicon. Polarizability assists in stabilizing charge through induced dipoles. Electron donation provides a similar role through induction and resonance. Because the empty orbital on silicon is 3p rather than 2p as is the case with carbocations, standard conjugation as in benzylic or allylic structures is considerably weakened. In fact, for phenyl the unfavorable

**Table 1.** NMR Parameters for Silylium Tetrakis(pentafluorophenyl)borates ( $R_3Si^+TPFPB^-$ )

$R_3$	solvent	$\delta(^{29}Si)$	$\Delta\delta(^{29}Si)^a$
Me <sub>3</sub>	C <sub>6</sub> D <sub>6</sub>	83.6	101.1
	none	84.8	
Et <sub>3</sub>	C <sub>6</sub> D <sub>6</sub>	92.3	92.1
	C <sub>6</sub> D <sub>6</sub> /C <sub>5</sub> H <sub>5</sub> CH <sub>3</sub> (3/1)	87.1	
	<i>p</i> -(CD <sub>3</sub> ) <sub>2</sub> C <sub>6</sub> H <sub>4</sub>	85.6	
	C <sub>6</sub> D <sub>5</sub> CD <sub>3</sub>	81.8	
	sulfolane	58.4	
	CD <sub>3</sub> CN	36.7	
iPr <sub>3</sub>	none <sup>b</sup>	94.3 <sup>c</sup>	95.5
	C <sub>6</sub> D <sub>6</sub>	107.5	
iBu <sub>3</sub>	none <sup>b</sup>	107.6	92.6
	C <sub>6</sub> D <sub>6</sub>	99.5	
MeiPr <sub>2</sub>	none <sup>b</sup>	89.4	96.8
	C <sub>6</sub> D <sub>6</sub>	96.9	
	CD <sub>3</sub> CN	41.9	
Hx <sub>3</sub>	pyridine/C <sub>6</sub> D <sub>6</sub>	44.3	96.8
	C <sub>6</sub> D <sub>6</sub>	90.3	
MePh <sub>2</sub>	mesitylene	65.	228.5
	C <sub>6</sub> D <sub>6</sub>	73.6	
(Me <sub>3</sub> Si) <sub>3</sub>	CD <sub>3</sub> CN	4.2	96.1
	C <sub>6</sub> D <sub>6</sub>	111.1	
	C <sub>6</sub> H <sub>5</sub> CH <sub>3</sub>	96.1	

<sup>a</sup>  $\delta(R_3Si^+TPFPB^-) - \delta(R_3SiH)$ . <sup>b</sup> Spectrum taken on solid samples in the absence of solvent with CP/MAS. <sup>c</sup> 93.5 when prepared in the presence of toluene.

**Table 2.** NMR Chemical Shifts for Isopropyl Methyl Groups in Methyl-diisopropylsilyl-X

X	solvent	$\delta(^1H)$	$\delta(^{13}C)$	status	
H	C <sub>6</sub> D <sub>6</sub>	0.97, 1.02	18.35, 18.99	diastereotopic	
	TPFPB	C <sub>6</sub> D <sub>6</sub>	0.58	16.74	homotopic
	CD <sub>3</sub> CN	0.93	12.26	homotopic	
ClO <sub>4</sub>	pyridine <sup>a</sup>	0.50	11.27	homotopic	
	C <sub>6</sub> D <sub>6</sub>	0.84, 0.89	16.33, 16.40	diastereotopic	
	CD <sub>2</sub> Cl <sub>2</sub>	1.10	16.67	homotopic	

<sup>a</sup> Made in the presence of C<sub>6</sub>D<sub>6</sub>, so the solvent was a mixture.

inductive effect of the sp<sup>2</sup> carbons may offset any effects of direct conjugation. Phenyl, however, also may stabilize charge by  $\pi$  polarization. The normally strong stabilization of charge by neighboring amine or ether functionalities through 2p conjugation likewise is offset by the inductive effects of nitrogen and oxygen. Thus herein we emphasize hydrocarbon substituents and those with atoms of low electronegativity such as silicon.

In the present study, we have combined the optimum choices of solvent, anion, and substituent in a series of experiments in both solution and solid states.

## Results

Trityl tetrakis(pentafluorophenyl)borate was prepared by the method of Chien et al.<sup>14</sup> and allowed to react with excess, dried silane without further solvent at room temperature in an inert atmosphere. The byproduct triphenylmethane was removed by washing the resulting solid with hexane. The washed solid was used directly for CP/MAS solid-state <sup>29</sup>Si and <sup>13</sup>C NMR experiments, was dissolved in a solvent for solution NMR, or was recrystallized from hexane/toluene mixtures for X-ray diffraction and NMR experiments. The purity of the product was monitored by <sup>1</sup>H, <sup>13</sup>C, and <sup>29</sup>Si NMR spectroscopies. Complete, clean reactions were obtained for trimethylsilyl, triethylsilyl, triisopropylsilyl, triisobutylsilyl, trihexylsilyl, methyl-diphenylsilyl, and methyl-diisopropylsilyl. The reaction of tris(trimethylsilyl)silyl also was complete but produced a simple mixture. Complex mixtures were

(9) Kira, M.; Hino, T.; Sakurai, H. *J. Am. Chem. Soc.* **1992**, *114*, 6697-6700.

(10) Bahr, S. R.; Boudjouk, P. *J. Am. Chem. Soc.* **1993**, *115*, 4514-4519.

(11) Lambert, J. B.; Zhang, S. *J. Chem. Soc., Chem. Commun.* **1993**, 383-384.

(12) Strauss, S. H. *Chem. Rev.* **1993**, *93*, 927-942.

(13) Xie, Z.; Liston, D. J.; Jekinek, R.; Mitro, V.; Bau, R.; Reed, C. A. *J. Chem. Soc., Chem. Commun.* **1993**, 384-386. Reed, C. A.; Xie, Z.; Bau, R.; Benesi, A. *Science* **1993**, *262*, 402-404. Reed, C. A.; Xie, Z. *Science* **1994**, *263*, 985-986.

(14) Chien, J. C. W.; Tsai, W.-M.; Rausch, M. D. *J. Am. Chem. Soc.* **1991**, *113*, 8570-8571.

(15) Yang, X.; Stern, C. L.; Marks, T. J. *Organometallics* **1991**, *10*, 840-842.

Table 3. Atomic Coordinates

atom <sup>a</sup>	x	y	z	B(eq), Å <sup>2</sup>	atom <sup>a</sup>	x	y	z	B(eq), Å <sup>2</sup>
Si1	0.2643(2)	0.7464(2)	0.3808(2)	2.7(2)	F39	0.6643(5)	0.2992(3)	0.3063(4)	4.4(5)
C2	0.271(1)	0.7620(7)	0.4802(6)	3.5(3)	F40	0.7325(5)	0.1532(3)	0.3427(3)	3.1(4)
C3	0.379(1)	0.7487(7)	0.5065(7)	4.3(3)	F47	0.8204(4)	0.0239(3)	0.1209(3)	2.8(4)
C4	0.346(1)	0.8062(7)	0.3177(7)	4.0(3)	F48	0.9163(5)	-0.0662(3)	0.0171(3)	3.9(4)
C5	0.319(1)	0.8913(8)	0.3361(7)	5.6(4)	F49	1.1043(6)	-0.1456(4)	0.0356(4)	5.9(5)
C6	0.1339(8)	0.7479(6)	0.3530(6)	3.0(3)	F50	1.1936(6)	-0.1317(4)	0.1629(4)	6.1(6)
C7	0.050(1)	0.7230(7)	0.4113(7)	4.3(3)	F51	1.1009(5)	-0.0440(3)	0.2665(3)	3.7(4)
C8	0.354(1)	0.6323(6)	0.3712(6)	2.9(3)	F58	1.0778(4)	0.1165(3)	0.2361(3)	3.2(4)
C9	0.2885(9)	0.5923(6)	0.4186(6)	2.9(3)	F59	1.1840(5)	0.1690(4)	0.3331(4)	4.5(5)
C10	0.2199(9)	0.5497(7)	0.3914(7)	3.6(3)	F60	1.1220(5)	0.1590(4)	0.4816(3)	4.3(5)
C11	0.2179(8)	0.5447(6)	0.3162(6)	2.5(2)	F61	0.9495(5)	0.0911(3)	0.5291(3)	3.1(4)
C12	0.2840(9)	0.5822(7)	0.2668(6)	3.4(3)	F62	0.8460(4)	0.0361(3)	0.4341(3)	2.5(4)
C13	0.3521(9)	0.6251(6)	0.2932(6)	3.1(3)	F69	0.6577(4)	0.0711(3)	0.2371(3)	3.2(4)
C14	0.145(1)	0.4980(7)	0.2880(7)	4.7(3)	F70	0.5268(5)	-0.0265(3)	0.2800(4)	4.0(4)
H1	0.2422	0.8135	0.4890	4.3	F71	0.5869(5)	-0.1605(3)	0.3589(3)	3.9(4)
H2	0.2301	0.7279	0.5089	4.3	F72	0.7864(5)	-0.1937(3)	0.3903(3)	3.3(4)
H3	0.4092	0.6974	0.4982	5.2	F73	0.9205(4)	-0.0945(3)	0.3481(3)	2.7(4)
H4	0.4206	0.7834	0.4795	5.2	C30	0.8414(8)	0.1381(6)	0.2321(5)	1.7(2)
H5	0.3752	0.7572	0.5580	5.2	C31	0.8774(8)	0.1748(6)	0.1675(6)	2.1(2)
H6	0.4164	0.7899	0.3241	4.8	C32	0.8422(8)	0.2522(6)	0.1485(6)	2.1(2)
H7	0.3339	0.8006	0.2677	4.8	C33	0.7723(9)	0.2927(7)	0.1944(6)	2.8(2)
H8	0.3302	0.8969	0.3863	6.7	C34	0.7336(9)	0.2596(7)	0.2594(6)	2.7(2)
H9	0.3612	0.9216	0.3042	6.7	C35	0.7706(8)	0.1827(6)	0.2765(6)	2.5(2)
H10	0.2486	0.9077	0.3291	6.7	C41	0.9555(8)	-0.0016(6)	0.1984(5)	1.8(2)
H11	0.1113	0.7991	0.3361	3.6	C42	0.9140(8)	-0.0132(6)	0.1340(6)	2.0(2)
H12	0.1387	0.7149	0.3129	3.6	C43	0.9636(9)	-0.0598(6)	0.0793(6)	2.5(2)
H13	0.0411	0.7560	0.4515	5.1	C44	1.058(1)	-0.0993(7)	0.0885(7)	3.4(3)
H14	-0.0133	0.7260	0.3893	5.1	C45	1.101(1)	-0.0921(7)	0.1515(7)	3.5(3)
H15	0.0695	0.6717	0.4291	5.1	C46	1.0505(8)	-0.0453(6)	0.2053(6)	2.4(2)
H16	0.2904	0.5938	0.4708	3.5	C52	0.9564(8)	0.0721(6)	0.3290(6)	1.8(2)
H17	0.1741	0.5240	0.4250	4.3	C53	1.0416(8)	0.1069(6)	0.3084(6)	2.1(2)
H18	0.2827	0.5786	0.2148	4.1	C54	1.0994(9)	0.1362(6)	0.3583(6)	2.6(2)
H19	0.3982	0.6500	0.2591	3.8	C55	1.0684(8)	0.1307(6)	0.4328(6)	2.5(2)
H20	0.0767	0.5175	0.3048	5.6	C56	0.9823(8)	0.0975(6)	0.4559(6)	2.2(2)
H21	0.1533	0.5006	0.2352	5.6	C57	0.9301(8)	0.0679(6)	0.4050(6)	1.9(2)
H22	0.1598	0.4461	0.3059	5.6	C63	0.7973(7)	-0.0045(5)	0.2933(5)	1.5(2)
H53	0.422(7)	0.659(5)	0.389(5)	4(2)	C64	0.6955(8)	0.0067(6)	0.2772(6)	1.9(2)
Si15	0.3950(3)	-0.7675(2)	0.1460(2)	3.4(2)	C65	0.6256(9)	-0.0437(6)	0.2975(6)	2.4(2)
C16	0.520(1)	-0.7354(7)	0.1150(6)	3.7(3)	C66	0.6546(8)	-0.1110(6)	0.3373(6)	2.3(2)
C17	0.608(1)	-0.7969(7)	0.0861(7)	4.7(3)	C67	0.7546(8)	-0.1265(6)	0.3543(6)	2.3(2)
C18	0.402(1)	-0.8474(8)	0.2187(8)	5.3(3)	C68	0.8220(8)	-0.0744(6)	0.3307(6)	2.1(2)
C19	0.441(1)	-0.8219(9)	0.2880(9)	7.1(4)	B29	0.889(1)	0.0492(7)	0.2632(7)	1.9(3)
C20	0.289(1)	-0.6888(7)	0.1663(6)	3.8(3)	F81	0.8084(4)	0.4263(3)	0.4044(3)	3.0(4)
C21	0.297(1)	-0.6110(7)	0.1272(7)	4.8(3)	F82	0.9318(5)	0.3018(3)	0.3647(4)	4.2(5)
C22	0.362(1)	-0.8257(8)	0.0507(8)	4.6(3)	F83	1.0376(5)	0.2973(4)	0.2276(4)	5.2(5)
C23	0.367(1)	-0.7661(8)	-0.0003(7)	4.5(3)	F84	1.0140(5)	0.4243(4)	0.1316(4)	4.7(5)
C24	0.283(1)	-0.7226(7)	-0.0257(7)	4.7(3)	F85	0.8913(5)	0.5476(3)	0.1688(3)	3.3(4)
C25	0.186(1)	-0.7422(8)	0.0019(7)	4.8(3)	F92	0.5778(4)	0.6718(3)	0.2502(3)	2.8(4)
C26	0.179(1)	-0.8025(8)	0.0512(8)	5.3(3)	F93	0.5918(5)	0.8054(3)	0.1784(3)	3.7(4)
C27	0.261(1)	-0.8468(8)	0.0773(7)	5.1(3)	F94	0.7758(5)	0.8612(3)	0.1508(3)	4.2(5)
C28	0.091(1)	-0.6947(9)	-0.0240(9)	7.5(4)	F95	0.9478(5)	0.7777(4)	0.2015(4)	4.6(5)
H23	0.5091	-0.6972	0.0759	4.4	F96	0.9360(4)	0.6427(3)	0.2760(3)	3.0(4)
H24	0.5424	-0.7132	0.1558	4.4	F103	0.6741(4)	0.5363(3)	0.1817(3)	2.6(4)
H25	0.6213	-0.8353	0.1245	5.7	F104	0.5223(5)	0.4557(3)	0.1652(3)	3.6(4)
H26	0.5876	-0.8197	0.0447	5.7	F105	0.4119(5)	0.3975(3)	0.2867(4)	3.9(4)
H27	0.6679	-0.7734	0.0715	5.7	F106	0.4587(5)	0.4234(3)	0.4241(3)	3.5(4)
H28	0.3359	-0.8626	0.2306	6.4	F107	0.6078(4)	0.5038(3)	0.4430(3)	2.5(4)
H29	0.4484	-0.8896	0.2002	6.4	F114	0.5987(4)	0.6637(3)	0.4050(3)	2.5(4)
H30	0.4457	-0.8636	0.3240	8.5	F115	0.6146(5)	0.7234(3)	0.5334(3)	3.6(4)
H31	0.5064	-0.8055	0.2759	8.5	F116	0.7901(5)	0.6916(3)	0.6034(3)	4.1(4)
H32	0.3937	-0.7806	0.3074	8.5	F117	0.9538(5)	0.6008(3)	0.5372(3)	3.6(4)
H33	0.2271	-0.7052	0.1534	4.6	F118	0.9419(4)	0.5421(3)	0.4092(3)	3.1(4)
H34	0.2831	-0.6821	0.2182	4.6	C75	0.8436(8)	0.4964(6)	0.2892(6)	1.8(2)
H35	0.3580	-0.5928	0.1392	5.7	C76	0.8580(8)	0.4299(6)	0.3360(6)	2.3(2)
H36	0.3005	-0.6154	0.0750	5.7	C77	0.9229(9)	0.3634(7)	0.3166(6)	2.7(2)
H37	0.2389	-0.5759	0.1428	5.7	C78	0.975(1)	0.3620(7)	0.2478(7)	3.3(3)
H38	0.4336	-0.7540	-0.0194	5.3	C79	0.9628(9)	0.4242(6)	0.2002(6)	2.5(2)
H39	0.2902	-0.6806	-0.0608	5.6	C80	0.8973(8)	0.4902(6)	0.2214(6)	2.5(2)
H40	0.1123	-0.8147	0.0686	6.3	C86	0.7570(8)	0.6477(6)	0.2657(5)	1.9(2)
H41	0.2536	-0.8895	0.1113	6.2	C87	0.6729(8)	0.6942(6)	0.2394(6)	2.0(2)
H42	0.0497	-0.6732	0.0176	9.0	C88	0.6783(9)	0.7653(6)	0.2026(6)	2.6(2)
H43	0.1101	-0.6545	-0.0580	9.0	C90	0.8551(9)	0.7510(6)	0.2135(6)	2.7(2)
H44	0.0526	-0.7264	-0.0477	9.0	C91	0.8485(9)	0.6804(6)	0.2517(6)	2.3(2)
H54	0.414(6)	-0.864(4)	0.068(4)	0(2)	C97	0.6495(7)	0.5265(5)	0.3124(5)	1.5(2)
F36	0.9499(4)	0.1399(3)	0.1184(3)	2.8(4)	C98	0.6208(8)	0.5113(6)	0.2454(6)	1.9(2)
F37	0.8841(5)	0.2843(3)	0.0843(3)	4.0(4)	C99	0.5432(8)	0.4684(6)	0.2353(6)	2.1(2)
F38	0.7380(5)	0.3666(3)	0.1752(4)	4.1(4)	C100	0.4877(8)	0.4402(6)	0.2954(6)	2.2(2)

Table 3 (Continued)

atom <sup>a</sup>	x	y	z	B(eq), Å <sup>2</sup>	atom <sup>a</sup>	x	y	z	B(eq), Å <sup>2</sup>
C101	0.5116(8)	0.4536(6)	0.3638(6)	2.1(2)	C122	0.692(1)	-0.7027(9)	-0.0971(8)	7.0(4)
C102	0.5909(8)	0.4956(5)	0.3711(6)	1.6(2)	C123	0.762(1)	-0.665(1)	-0.0682(9)	7.4(4)
C108	0.7684(8)	0.5964(6)	0.4011(6)	2.0(2)	C124	0.721(1)	-0.5939(8)	-0.0336(7)	5.2(3)
C109	0.6890(8)	0.6461(6)	0.4363(6)	1.9(2)	C125	0.792(1)	-0.550(1)	0.0004(9)	7.7(4)
C110	0.6961(8)	0.6777(6)	0.5030(6)	2.2(2)	C200	0.416(1)	-0.038(1)	0.516(1)	7.8(4)
C111	0.7830(8)	0.6632(6)	0.5373(6)	2.2(2)	C201	0.402(1)	0.039(1)	0.483(1)	7.7(5)
C112	0.8639(9)	0.6163(6)	0.5055(6)	2.3(2)	C202	0.505(2)	-0.075(1)	0.533(1)	8.1(5)
C113	0.8565(9)	0.5865(6)	0.4376(6)	2.2(2)	C203	0.329(2)	0.073(1)	0.460(1)	4.5(6)
B74	0.755(1)	0.5663(7)	0.3181(7)	2.1(3)	H45	0.5913	-0.5210	-0.0206	7.1
C300	0.441(1)	0.013(1)	0.941(1)	7.3(4)	H46	0.4852	-0.5892	-0.0763	7.8
C301	0.603(1)	0.020(1)	0.999(1)	8.9(5)	H47	0.5501	-0.7071	-0.1251	8.2
C302	0.537(2)	0.035(1)	0.936(1)	9.0(5)	H48	0.7172	-0.7518	-0.1154	8.4
C303	0.391(3)	-0.057(2)	1.098(2)	10(1)	H49	0.8336	-0.6847	-0.0706	8.9
C119	0.620(1)	-0.5689(8)	-0.0401(8)	5.9(4)	H50	0.8581	-0.5788	-0.0004	9.2
C120	0.555(1)	-0.609(1)	-0.0734(8)	6.5(4)	H51	0.7960	-0.5024	-0.0271	9.2
C121	0.593(1)	-0.678(1)	-0.1023(8)	6.8(4)	H52	0.7658	-0.5406	0.0502	9.2

<sup>a</sup> Atoms are identified in Figures 3-6.

Table 4. Intramolecular Distances (Å)<sup>a</sup>

Si1-C2	1.85(1)	F38-C33	1.35(1)	C52-C53	1.36(1)	F117-C112	1.35(1)
Si1-C4	1.86(1)	F39-C34	1.34(1)	C52-C57	1.38(1)	F118-C113	1.36(1)
Si1-C6	1.83(1)	F40-C35	1.35(1)	C52-B29	1.65(1)	C75-C76	1.40(1)
Si1-C8	2.19(1)	F47-C42	1.35(1)	C53-C54	1.40(1)	C75-C80	1.36(1)
C2-C3	1.54(1)	F48-C43	1.36(1)	C54-C55	1.37(1)	C75-B74	1.65(2)
C4-C5	1.54(2)	F49-C44	1.34(1)	C55-C56	1.36(1)	C76-C77	1.39(1)
C6-C7	1.54(2)	F50-C45	1.35(1)	C56-C57	1.37(1)	C77-C78	1.36(1)
C8-C9	1.38(1)	F51-C46	1.35(1)	C63-C64	1.39(1)	C78-C79	1.35(1)
C8-C13	1.43(1)	F58-C53	1.36(1)	C63-C68	1.38(1)	C79-C80	1.40(1)
C9-C10	1.39(1)	F59-C54	1.35(1)	C63-B29	1.66(1)	C86-C87	1.39(1)
C10-C11	1.37(1)	F60-C55	1.35(1)	C64-C65	1.37(1)	C86-B74	1.67(1)
C11-C12	1.38(1)	F61-C56	1.36(1)	C65-C66	1.37(1)	C87-C88	1.38(1)
C11-C14	1.49(1)	F62-C57	1.35(1)	C66-C67	1.37(1)	C88-C89	1.34(1)
C12-C13	1.39(1)	F69-C64	1.37(1)	C67-C68	1.38(1)	C89-C90	1.35(1)
C8-H53	1.15(8)	F70-C65	1.36(1)	F81-C76	1.34(1)	C90-C91	1.39(1)
Si15-C16	1.83(1)	F71-C66	1.34(1)	F82-C77	1.34(1)	C97-C98	1.36(1)
Si15-C18	1.86(1)	F72-C67	1.35(1)	F83-C78	1.36(1)	C97-C102	1.38(1)
Si15-C20	1.86(1)	F73-C68	1.36(1)	F84-C79	1.35(1)	C97-B74	1.65(1)
Si15-C22	2.17(1)	C30-C31	1.37(1)	F85-C80	1.34(1)	C98-C99	1.38(1)
C16-C17	1.55(2)	C30-C35	1.37(1)	F92-C87	1.35(1)	C99-C100	1.35(1)
C18-C19	1.52(2)	C30-B29	1.69(1)	F93-C88	1.35(1)	C100-C101	1.35(1)
C20-C21	1.51(2)	C31-C32	1.41(1)	F94-C89	1.37(1)	C101-C102	1.38(1)
C22-C23	1.35(2)	C32-C33	1.34(1)	F95-C90	1.36(1)	C108-C109	1.40(1)
C22-C27	1.45(2)	C33-C34	1.36(1)	F96-C91	1.35(1)	C108-C113	1.38(1)
C23-C24	1.36(2)	C34-C35	1.40(1)	F103-C98	1.37(1)	C108-B74	1.66(1)
C24-C25	1.41(2)	C41-C42	1.38(1)	F104-C99	1.37(1)	C109-C110	1.38(1)
C25-C26	1.35(2)	C41-C46	1.39(1)	F105-C100	1.36(1)	C110-C111	1.34(1)
C25-C28	1.51(2)	C41-B29	1.63(2)	F106-C101	1.35(1)	C111-C112	1.36(1)
C26-C27	1.35(2)	C42-C43	1.38(1)	F107-C102	1.36(1)	C112-C113	1.39(1)
C22-H54	0.95(7)	C43-C44	1.36(1)	F114-C109	1.36(1)		
F36-C31	1.35(1)	C44-C45	1.35(1)	F115-C110	1.35(1)		
F37-C32	1.36(1)	C45-C46	1.38(1)	F116-C111	1.34(1)		

<sup>a</sup> Atoms are identified in Figures 3-6.

obtained with triphenylsilyl, dimethyl[(trimethylsilyl)methyl]silyl, diphenyl[(trimethylsilyl)methyl]silyl, ethyldimethylsilyl, tri-*tert*-butylsilyl, and cyclohexyldi-*tert*-butylsilyl.

Triethylsilylium tetrakis(pentafluorophenyl)borate was selected for more intensive study in a variety of solvents, and methyl-diphenylsilylium tetrakis(pentafluorophenyl)borate was examined in three solvents. The other substrates were examined only in benzene or toluene. Table 1 lists all the <sup>29</sup>Si NMR data. Substrates that produced complex mixtures invariably exhibited no downfield resonance. The tris(trimethylsilyl)silyl substrate was particularly sensitive to oxygen and hydrolysis and, in addition to the downfield peak, produced one or two other <sup>29</sup>Si resonances further upfield. Triethylsilylium tetrakis(pentafluorophenyl)borate was insoluble in hexamethylbenzene and hexafluorobenzene and reacted with dichloromethane and sulfur dioxide. Boron-11 spectra were

identical for all examined substrates in solution, including trityl tetrakis(pentafluorophenyl)borate, with a single peak at  $\delta$  -20 and a line width of about 20 Hz. Likewise the solution <sup>19</sup>F spectra of all species contained the same three peaks (within  $\pm 0.1$  ppm), at  $\delta$  -166.6 (ortho), -132.3 (meta), and -162.6 (para). The electronic spectrum for triethylsilylium contained a single broad peak with a maximum at 303 nm in benzene.

In light of the mixture for the case of tris(trimethylsilyl)silane, the reaction also was carried out at -20 °C for product analysis. The silylium borate was allowed to react with diBALH, tris(trimethylsilyl)silane was isolated in >25% yield, and its structure was proved by gas chromatography and mass spectrometry.

A special substrate was synthesized in order to probe the symmetry of the silylium ions. The isopropyl methyl groups of methyl-diisopropylsilane (Me(iPr)<sub>2</sub>SiH) are diastereotopic and nonequivalent both in the <sup>1</sup>H and in the

Table 5. Intramolecular Bond Angles (deg)<sup>a</sup>

C2-Si1-C4	112.8(5)	C30-C31-C32	122(1)	C68-C63-B29	119.9(9)	C88-C89-C90	120(1)
C2-Si1-C6	114.9(5)	F37-C32-C31	118(1)	F69-C64-C63	120.6(9)	F95-C90-C89	121(1)
C2-Si1-C8	101.0(5)	F37-C32-C33	122(1)	F69-C64-C65	114.5(9)	F95-C90-C91	119(1)
C4-Si1-C6	113.7(5)	C31-C32-C33	120(1)	C63-C64-C65	125(1)	C89-C90-C91	120(1)
C4-Si1-C8	101.0(5)	F38-C33-C32	120(1)	F70-C65-C64	120(1)	F96-C91-C86	119.5(9)
C6-Si1-C8	111.7(5)	F38-C33-C34	120(1)	F70-C65-C66	120(1)	F96-C91-C90	117(1)
Si1-C2-C3	115.1(9)	C32-C33-C34	121(1)	C64-C65-C66	120(1)	C86-C91-C90	123(1)
Si1-C4-C5	109.6(9)	F39-C34-C33	122(1)	F71-C66-C65	121(1)	C98-C97-C102	112.6(9)
Si1-C6-C7	118.5(8)	F39-C34-C35	121(1)	F71-C66-C67	121(1)	C98-C97-B74	120.9(9)
Si1-C8-C9	97.1(8)	C33-C34-C35	118(1)	C65-C66-C67	118(1)	C102-C97-B74	125.8(9)
Si1-C8-C13	98.8(8)	F40-C35-C30	120(1)	F72-C67-C66	120(1)	F103-C98-C97	119.4(9)
Si1-C8-C11	104(1)	F40-C35-C34	115(1)	F72-C67-C68	121(1)	F103-C98-C99	115.5(9)
Si1-C8-H53	87(4)	C30-C35-C34	125(1)	C66-C67-C68	119(1)	C97-C98-C99	125(1)
C9-C8-C13	117(1)	C42-C41-C46	113(1)	F73-C68-C63	118.5(9)	F104-C99-C98	119.9(9)
C9-C8-H53	124(5)	C42-C41-B29	121(1)	F73-C68-C67	115.7(9)	F104-C99-C100	120.7(9)
C8-C9-C10	121(1)	C46-C41-B29	125.1(9)	C63-C68-C67	126(1)	C98-C99-C100	119(1)
C13-C8-H53	117(5)	F47-C42-C41	120(1)	C30-B29-C41	113.3(9)	F105-C100-C99	120(1)
C9-C10-C11	120(1)	F47-C42-C43	116.5(9)	C30-B29-C52	99.6(8)	F105-C100-C101	121(1)
C10-C11-C12	120(1)	C41-C42-C43	124(1)	C30-B29-C63	112.4(9)	C99-C100-C101	119(1)
C10-C11-C14	120(1)	F48-C43-C42	119(1)	C41-B29-C52	115.3(9)	F106-C101-C100	119(1)
C12-C11-C14	120(1)	F48-C43-C44	121(1)	C41-B29-C63	102.4(8)	F106-C101-C102	121.2(9)
C11-C12-C13	120(1)	C42-C43-C44	120(1)	C52-B29-C63	114.4(9)	C100-C101-C102	120(1)
C8-C13-C12	121(1)	F49-C44-C43	119(1)	C76-C75-C80	114(1)	F107-C102-C97	121.8(9)
C16-Si15-C18	113.6(6)	F49-C44-C45	122(1)	C76-C75-B74	117(1)	F107-C102-C101	113.8(9)
C16-Si15-C20	114.8(5)	C43-C44-C45	119(1)	C80-C75-B74	128(1)	C97-C102-C101	124(1)
C16-Si15-C22	102.6(6)	F50-C45-C44	120(1)	F81-C76-C75	121(1)	C109-C108-C113	113(1)
C18-Si15-C20	114.1(6)	F50-C45-C46	120(1)	F81-C76-C77	115(1)	C109-C108-B74	119.5(9)
C18-Si15-C22	101.5(6)	C44-C45-C46	120(1)	C75-C76-C77	124(1)	C113-C108-B74	127(1)
C20-Si15-C22	108.6(6)	F51-C46-C41	121(1)	F82-C77-C76	120(1)	F114-C109-C108	119.4(9)
Si15-C16-C17	117.3(8)	F51-C46-C45	115(1)	F82-C77-C78	121(1)	F114-C109-C110	117(1)
Si15-C18-C19	110(1)	C41-C46-C45	124(1)	C76-C77-C78	119(1)	C108-C109-C110	123(1)
Si15-C20-C21	117.8(9)	C53-C52-C57	114(1)	F83-C78-C77	119(1)	F115-C110-C109	119(1)
Si15-C22-C23	97.6(9)	C53-C52-B29	118.4(9)	F83-C78-C79	121(1)	F115-C110-C111	120(1)
Si15-C22-C27	100.0(9)	C57-C52-B29	127.3(9)	C77-C78-C79	120(1)	C109-C110-C111	121(1)
Si15-C22-C25	105(1)	F58-C53-C52	122(1)	F84-C79-C78	121(1)	F116-C111-C110	121(1)
Si15-C22-H54	82(4)	F58-C53-C54	114.1(9)	F84-C79-C80	119(1)	F116-C111-C112	120(1)
C23-C22-C27	118(1)	C52-C53-C54	124(1)	C78-C79-C80	120(1)	C110-C111-C112	119(1)
C23-C22-H54	132(5)	F59-C54-C53	120(1)	F85-C80-C75	122(1)	F117-C112-C111	121(1)
C22-C23-C24	124(1)	F59-C54-C55	121(1)	F85-C80-C79	114(1)	F117-C112-C113	119(1)
C27-C22-H54	109(5)	C53-C54-C55	119(1)	C75-C80-C79	124(1)	C111-C112-C113	120(1)
C23-C24-C25	117(1)	F60-C55-C54	120(1)	C87-C86-C91	113(1)	F118-C113-C108	120(1)
C24-C25-C26	120(1)	F60-C55-C56	121(1)	C87-C86-B74	127(1)	F118-C113-C112	115.6(9)
C24-C25-C28	119(1)	C54-C55-C56	119(1)	C91-C86-B74	119.8(9)	C108-C113-C112	124(1)
C26-C25-C28	121(1)	F61-C56-C55	121(1)	F92-C87-C86	120.4(9)	C75-B74-C86	113.5(9)
C25-C26-C27	124(1)	F61-C56-C57	119.5(9)	F92-C87-C88	115.5(9)	C75-B74-C97	100.4(8)
C22-C27-C26	117(1)	C55-C56-C57	120(1)	C86-C87-C88	124(1)	C75-B74-C108	114.7(9)
C31-C30-C35	115(1)	F62-C57-C52	121.0(9)	F93-C88-C87	119(1)	C86-B74-C97	112.4(9)
C31-C30-B29	125(1)	F62-C57-C56	114.9(9)	F93-C88-C89	121(1)	C86-B74-C108	101.0(8)
C35-C30-B29	120.1(9)	C52-C57-C56	124(1)	C87-C88-C89	120(1)	C97-B74-C108	115.4(9)
F36-C31-C30	123(1)	C64-C63-C68	111.9(9)	F94-C89-C88	120(1)		
F36-C31-C32	115.4(9)	C64-C63-B29	127.5(9)	F94-C89-C90	120(1)		

<sup>a</sup> Atoms are identified in Figures 3-6.

<sup>13</sup>C spectra. If the silylium ion is statically nonplanar, as in a tetracoordinate structure in which solvent provides the fourth coordination, the methyls would be diastereotopic. Observation of diastereotopicity therefore is *prima facie* evidence for tetracoordination. On the other hand, a tricoordinate silylium ion or a tetracoordinate solvent complex in which solvent is exchanging faster than the NMR time scale would have homotopic methyl groups that are equivalent in the <sup>1</sup>H and <sup>13</sup>C spectra. Table 2 gives the results for both methylidisopropylsilylium tetrakis(pentafluorophenyl)borate and methylidisopropylsilylium perchlorate in a variety of solvents.

Crystals of triethylsilylium tetrakis(pentafluorophenyl)borate that had been recrystallized from hexane/toluene were analyzed by X-ray diffraction. Table 3 provides the atomic coordinates of the resulting structure, and Tables 4 and 5 contain structural parameters. Figure 1 illustrates the unit cell, and Figure 2 contains one fundamental grouping of triethylsilylium, TPFPB, and toluene. Figures 3-6 provide the atomic numbering sequence.

## Discussion

**Ions in Solution.** In all cases, there appears to be little interaction between the cation and the anion, or at least no more significant interaction for the silyl cations than for the precursor carbocation (trityl). The identities of the <sup>11</sup>B chemical shift and line width indicate that the borate anion experiences little or no alteration from perfect tetrahedral symmetry (as a quadrupolar nucleus, <sup>11</sup>B would give broadened and shifted resonances with deviations from tetrahedrality). Moreover, the <sup>19</sup>F chemical shifts are unchanged on going from trityl to silylium. We expected that the well-known strength of the Si-F interaction might be manifested in this context. Even when the fact that there are four *para* positions or eight *ortho/meta* positions is taken into consideration, the lack of any change in the <sup>19</sup>F shift strongly suggests that the fluorines on the anion are not interacting with the silicon of the cation. These fluorine atoms reside on the *sp*<sup>2</sup> atoms of the benzene rings and donate electrons to the aromatic rings (C=F<sup>+</sup>), thereby reducing their silaphilicity. They

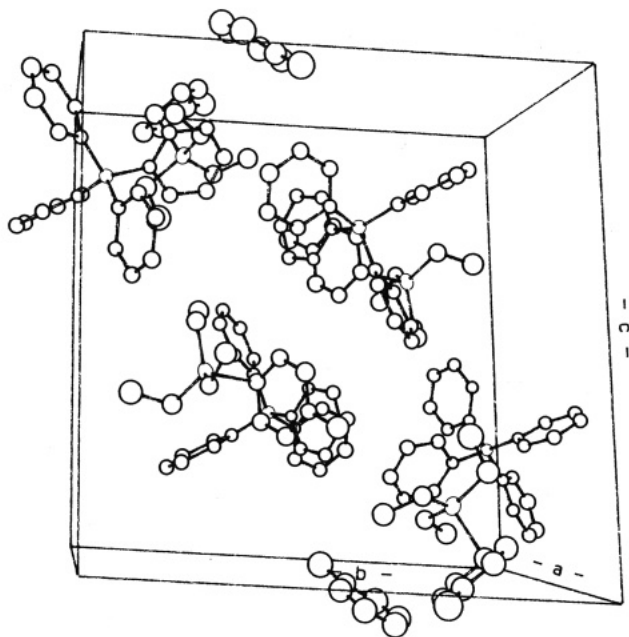


Figure 1. Unit cell of  $[\text{Et}_3\text{Si}][\text{TPFPB}]\cdot 2\text{toluene}$ .

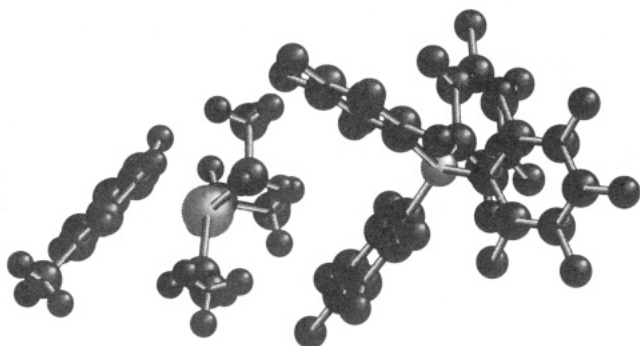


Figure 2. Juxtaposition of the triethylsilylium cation, the TFPBPB anion, and the coordinated toluene.

are quite different fluorines from those on the tetrakis-[bis(3,5-trifluoromethyl)phenyl]borate anion studied by Sakurai<sup>9</sup> and Boudjouk.<sup>10</sup> As these latter fluorines are attached to  $\text{sp}^3$  atoms, they are more able to bind to silicon, but more importantly they are prone to abstraction to produce a benzylic cation and hence lead to decomposition. We have found the TFPBPB anion to be quite stable at room temperature for days in a variety of solvents containing silylium ions.

The  $^{29}\text{Si}$  figures in Table 1, particularly for triethylsilylium, show a gradation of interactions with solvent. We expected highly nucleophilic solvents such as pyridine, triethylamine, triphenylphosphine oxide, or HMPA to complex strongly with silicon. With triethylsilylium we began our study with the much less nucleophilic acetonitrile. The  $\delta$  value of 36.7 is normal for tetracoordinate species and represents a shift of only 30.7 ppm from the silane standard ( $\text{Et}_3\text{SiH}$ ). In the more weakly coordinating sulfolane, there is a further downfield shift of 22 ppm to  $\delta$  58.4. The trend continues to the even less nucleophilic aromatic hydrocarbons, but within this latter series there are some unexpected observations. The donor ability, by any measure such as ionization potential, is benzene < toluene < *p*-xylene. Indeed, benzene is least complexing and gives rise to a chemical shift of  $\delta$  92.3. The better donor toluene gives a complex that resonates at  $\delta$  81.8. The donor-acceptor interaction, however, is sensitive not

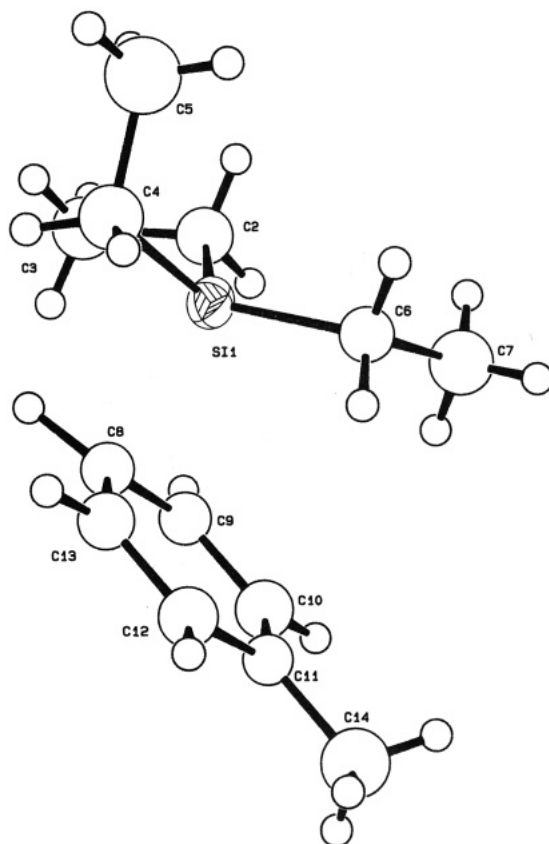


Figure 3. Numbering for first triethylsilylium and coordinated toluene.

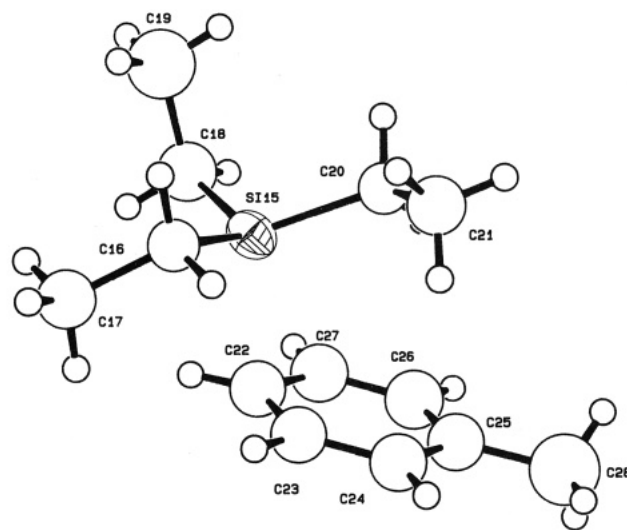


Figure 4. Numbering for second triethylsilylium and coordinated toluene.

only to the nucleophilicity of the donor but also to steric interactions between donor and acceptor. We believe that the steric effect of the additional methyl group of *p*-xylene more than offsets the increment in donor ability provided by the methyl group, so that its chemical shift is intermediate,  $\delta$  85.6. The larger steric effect weakens the donor-acceptor interaction and results in a downfield shift with respect to toluene. We attempted to follow this trend further, to hexamethylbenzene, but the more sterically hindered arenes were not successful solvents. The additional saturated hydrocarbon portions apparently prevented dissolution of the ions. A mixture of toluene and benzene also gives an intermediate value,  $\delta$  87.1. *The*



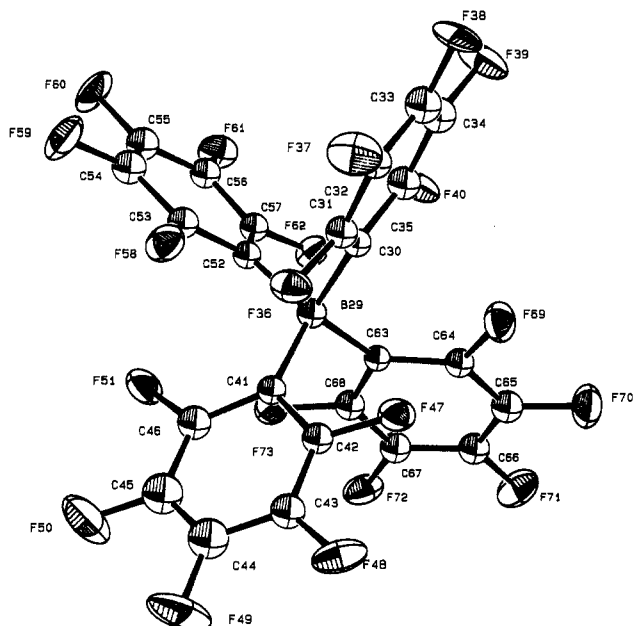


Figure 5. Numbering for first TPFPB.

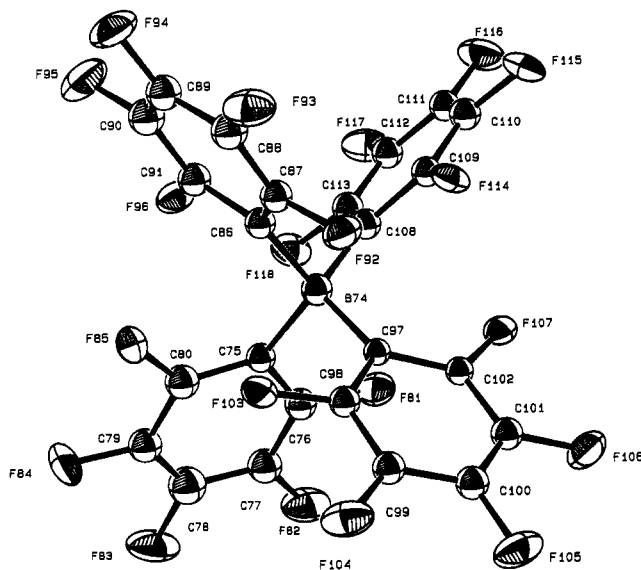


Figure 6. Numbering for second TPFPB.

observation of a single peak in the mixed solvent means that binding and dissociation between solvent and silylium are fast on the NMR time scale.

It is clear from the data for triethylsilylium that there is a gradation in complexation. Thus the downfield shift might reflect a shift in equilibrium (eq 3) from complexed to free silyl cations (two species), or more likely, it might reflect a loosening of the donor–acceptor interaction within a single species. In either case, the silyl species moves toward a structurally free silylium ion as the solvent donor ability decreases. It is the variability of the interaction that we want to emphasize. It is also clear that these species do not yet represent a fully free silyl cation, as chemical shifts in the range  $\delta$  80–110 are still some 200 ppm from the expected value for a free silyl cation.<sup>16</sup>

(16) Olah, G. A.; Field, L. D. *Organometallics* 1982, 1, 1485–1487. Schindler, cited in footnote 18 of: Olah, G. A.; Heiliger, L.; Li, X.-Y.; Surya Prakash, G. K. *J. Am. Chem. Soc.* 1990, 112, 5991–5995. Olah, G. A.; Rasul, G.; Heiliger, L.; Bausch, J.; Surya Prakash, G. K. *J. Am. Chem. Soc.* 1992, 114, 7737–7742. Olah, G. A.; Rasul, G.; Li, X.-Y.; Buchholz, H. A.; Sandford, G.; Surya Prakash, G. K. *Science* 1994, 263, 983–984.

At present the lower limit to the chemical shift is observed with triisopropylsilylium ( $\delta$  107.5 in benzene), but this value reflects the normal  $\beta$  chemical shift effects of the added methyl groups. As these  $\beta$  effects also are observed in the starting silane, the difference in chemical shift ( $\Delta\delta$ ) between the TPFPB salt and the silane provides a more accurate measure of the change in coordination. By this measure, there is not a lot of difference (ppm) among  $\text{Me}_3\text{Si}$  (101.1),  $\text{Et}_3\text{Si}$  (92.1),  $\text{iPr}_3\text{Si}$  (95.5),  $\text{iBu}_3\text{Si}$  (99.5),  $\text{MeiPr}_2\text{Si}$  (92.6), and  $\text{Hex}_3\text{Si}$  (96.8), all in benzene. There is, however, an extraordinary difference for the case of  $(\text{Me}_3\text{Si})_3\text{Si}$ , for which  $\Delta\delta$  is 228.5 ppm. The very strong upfield  $\alpha$  effect of the trimethylsilyl group is entirely offset by the unprecedented downfield effect of the change in coordination. The trimethylsilyl group thus provides the closest approach to perfect tricoordination. This group is successful for both electronic and steric reasons. Its high polarizability should be very effective in stabilizing the positive charge through induced dipoles. Moreover, the large size of the groups should assist in preventing the close approach of solvent, an effect that we also had tried to achieve with *tert*-butyl and mesityl groups.

Some measure of the strength of the solvent–silicon interaction can be obtained by the use of methyldiisopropylsilane, the results for which are given in Table 2. The methyl groups in each isopropyl group of this silane are diastereotopic and give separate  $^1\text{H}$  and  $^{13}\text{C}$  resonances. On conversion to the TPFPB salt, the methyl groups become homotopic in benzene, acetonitrile, and pyridine. Given the large chemical shift difference for the silane and the equivalence for both  $^1\text{H}$  and  $^{13}\text{C}$  in three different solvents, it is unlikely that the homotopicity is accidental. It is more likely that the methyl groups become equivalent by rapid exchange on the NMR time scale.

If this exchange is dissociative, as in the reverse of eq 3, then an upper limit of about 13 kcal mol<sup>-1</sup> may be set for this process in all solvents, with a progressively smaller value in the less coordinating solvents, benzene being at the extreme low end. The value of 13 kcal mol<sup>-1</sup> is obtained from  $k_c = \pi(\Delta\nu)/2^{1/2}$  and  $\Delta G_c^* = 2.3RT_c(10.32 + (\log T_c)/k_c)$  with  $\Delta\nu = 20$  Hz and  $T_c = 273$  K. The value can be no higher, as  $\Delta\nu$  cannot increase appreciably (Table 2) and  $T_c$ , if anything, is lower than 273 K, but the value can be much lower, depending on  $T_c$ . Variable-temperature experiments were prohibited by the limited solubility of these ions in the aromatic solvents. In other solvents, no changes were seen with lowered temperatures.

For the case of nitriles, rapid exchange on the NMR time scale also has been observed by Boudjouk<sup>10</sup> and Tilley<sup>17</sup> and their co-workers. Equivalence also may be attained with an associative mechanism, since the diastereotopic methyl groups would become equivalent in a trigonal bipyramid with two solvent molecules in the apical positions. Both Boudjouk and Tilley, however, present arguments against the associative mechanism for the case of nitrile exchange. These experiments suggest the binding between silicon and solvent (or anion) in these complexes has a very low bond order, corresponding to a dissociation energy of no more than 13 kcal mol<sup>-1</sup>.

We also examined conversion of this same silane to its perchlorate salt, as we accumulated considerable data previously on this anion.<sup>8</sup> As Table 2 indicates, the methyl

(17) Straus, D. A.; Zhang, C.; Quimbita, G. E.; Grumbine, S. D.; Heyn, R. H.; Tilley, T. D.; Rheingold, A. L.; Geib, S. J. *J. Am. Chem. Soc.* 1990, 112, 2673–2681.

groups are diastereotopic in benzene but homotopic in dichloromethane (a solvent we could not use with the TFPFB anion). The homotopicity in  $\text{CH}_2\text{Cl}_2$  is consistent with the ionic formation based on conductance and cryoscopy<sup>8</sup> and is inconsistent with the fully covalent formulation of Olah et al.<sup>16</sup> We had not previously examined any perchlorate in benzene. The diastereotopicity in this solvent contrasts both with the observation of the perchlorate in dichloromethane and with the observations of the TFPFB salts in all other solvents. On the one hand, the nonequivalence indicates tighter binding (an ion pair or a covalent structure) in the less polar benzene than in dichloromethane. On the other hand, the nonequivalence corroborates that the equivalences observed for the TFPFB salts were not accidental.

The energy for association of toluene with  $\text{Me}_3\text{Si}^+$  in the gas phase has been measured mass spectrometrically to be 28.4 kcal mol<sup>-1</sup>.<sup>18</sup> This figure should be considered an upper limit in solution, since ionic solvation would serve to stabilize the free ion. Although we cannot assess the exact energy of the interaction between the silyl cation and these solvents, arenes in particular, this upper limit in the gas phase and the observation that exchange between the cation and solvent is fast on the NMR time scale indicate that binding is a fraction (10–30 kcal mol<sup>-1</sup>) of that in a fully covalent C–Si bond, for which the bond dissociation energy is 90 kcal mol<sup>-1</sup>.<sup>19</sup> Such binding may reflect weak covalent bonding, but in energy it more closely resembles noncovalent interactions such as a hydrogen bond or an electrostatic bond like that between  $\text{Cl}^+$  and the  $\pi$  cloud of benzene.

**Ions in the Solid.** For solid-state NMR studies, conversion of trityl tetrakis(pentafluorophenyl)borate to silylium tetrakis(pentafluorophenyl)borate was accomplished by exposure of the solid trityl salt to excess silane. The heterogeneous reaction resulted in complete conversion of the silane to the silyl salt for those cases reported, as determined by <sup>1</sup>H NMR spectroscopy. The silyl salt was washed with hexane to remove the triphenylmethane byproduct, and the resulting material was packed into the rotor in a glovebox for examination by cross polarization, magic angle spinning methods.

As indicated by the data in Table 1, the chemical shifts (ppm) in the solid state are very similar to those in benzene solution: 83.6 vs 84.8 for  $\text{Me}_3\text{Si}$ , 92.3 vs 94.3 for  $\text{Et}_3\text{Si}$ , 107.5 vs 107.6 for  $i\text{Pr}_3\text{Si}$ , and 99.5 vs 89.4 for  $i\text{Bu}_3\text{Si}$ . Thus the extent of the fourth coordination must be very similar in the two states, even though the identity of the ligand may be quite different. The solution data of Table 1 indicate that the <sup>29</sup>Si chemical shift is in fact quite sensitive to the identity of the fourth ligand (see data for  $\text{Et}_3\text{Si}$ ). Thus it must be a coincidence that the (unspecified) ligand in the solid state provides a degree of coordination similar to that of benzene in solution. It is possible that the anion, in the absence of any solvent, coordinates through one or two fluorine atoms, as was observed for this anion by Marks et al.<sup>15</sup> It is less likely that the starting silane coordinates with silicon through interaction with a Si–H or Si–C bond or with the very electron-deficient  $\pi$  bonds of the aromatic rings of the anion.

The material used for X-ray analysis was prepared in the usual fashion and recrystallized from a mixture of

toluene and hexane. The crystals were sensitive to moisture but were handled only under inert atmosphere or oil and were extremely robust to the X-ray experiment, surviving 5 days of radiation without change. The unit cell (Figure 1) contains four sets of  $[\text{Et}_3\text{Si}][\text{B}(\text{C}_6\text{F}_5)_4] \cdot 2$ -toluene, made up of two crystallographically distinct pairs. Within each pair the sets are related by a center of inversion. Thus the data in Tables 3–5 contain two complete sets of structural parameters. There are no significant structural differences between the crystallographically distinct pairs, so we use the averages from the pairs throughout this discussion. Each inversion pair contains four toluene molecules. Two of these are weakly coordinated to the respective silicon atoms (one with each) and will be discussed in detail below. A third, in which the carbons are labeled C119–C125 and the hydrogens H45–H52 in Table 3, is entirely uncoordinated. In addition, there are two uncoordinated half-toluenes. Viewed as a whole, this last toluene is reorienting within the crystal, so that the methyl group is averaged with a position that contains only a substituent hydrogen. The carbons are labeled C201–C203 in one reorienting toluene and C300–C303 in the other. These entirely uncoordinated toluenes will not be considered further. The reorientation of the half-toluenes contributes to an increased *R* factor (0.069).

Possibly the most significant aspect of the structure is the complete lack of coordination of the anion. Silicon and fluorine normally form an extremely strong bond, and it was expected that there might be important nonbonding interactions between the fluorines on the anion and the silicon on the cation. In fact, the closest approach is 4.02 Å, well beyond the sum of the van der Waals radii. There is no indication of the chelating interaction of two fluorines that was observed by Marks et al. to thorium.<sup>15</sup> The considerable distance between cation and anion makes it difficult or arbitrary even to assign which are paired together within the unit cell. Figure 2 presents the triethylsilyl group between the toluene and the anion, and we have previously illustrated the grouping alternatively with toluene between triethylsilyl and the anion,<sup>20</sup> i.e., as a solvent-separated ion pair.

The second most striking aspect of the structure is the unprecedented distance between silicon and the fourth coordination site, the solvent toluene. The geometry of this interaction is clearly  $\eta^1$  rather than  $\eta^2$  or  $\eta^6$ . The distance of 2.18 Å is to be compared with the longest C–Si bond that we have been able to find, 2.03 Å in the extremely crowded four-membered ring  $[-(t\text{-Bu})_2\text{Si}(t\text{-Bu}_2\text{Si})\text{O}(\text{CPh}_2)-]$ .<sup>21</sup> A compilation of C–Si bond lengths<sup>22</sup> contains a number of such long C–Si bonds in the range 1.90–2.03 Å and of normal C–Si bonds in the range 1.81–1.87 Å with a mean of 1.845 Å (20 values). The observed value of 2.18 Å is 0.3 Å longer than the sum of the C and Si covalent radii (1.88 Å)<sup>22</sup> but still much shorter than the sum of the van der Waals radii. This long distance may be compared with three structures reported recently by Reed and co-workers,<sup>13</sup> respectively  $i\text{Pr}_3\text{Si}$  bound to an acetonitrile molecule and to the anion (*closo*- $\text{CB}_9\text{H}_5\text{Br}_5^-$  or *closo*-

(20) Lambert, J. B.; Zhang, S.; Stern, C. L.; Huffman, J. C. *Science* 1993, 260, 1917–1918. Lambert, J. B.; Zhang, S. *Science* 1994, 263, 984–985.

(21) Schäfer, A.; Weidenbruch, M.; Pohl, S. *J. Organomet. Chem.* 1985, 282, 305–313.

(22) Sheldrick, W. S. In *The Chemistry of Organic Silicon Compounds*; Patai, S., Rappoport, Z., Eds.; Wiley: Chichester, U.K., 1983; Part 1, p 246.

(18) Stone, J. M.; Stone, J. A. *Int. J. Mass Spectrom. Ion Processes* 1991, 109, 247–000.

(19) Walsh, R. In *The Chemistry of Organic Silicon Compounds*; Patai, S., Rappoport, Z., Eds.; Wiley: Chichester, U.K., 1989; Part 1, p 385.



Table 6. Bond Orders for R<sub>3</sub>Si-L

R	L	anion	Si-L(obs), Å	Si-L(n = 1), <sup>a</sup> Å	n	ref
Et	toluene	TPFPB <sup>-</sup>	2.18	1.85	0.28	present work
iPr	<i>closo</i> -CB <sub>11</sub> H <sub>6</sub> Br <sub>6</sub> <sup>-</sup>		2.48	2.24	0.40	13
iPr	<i>closo</i> -CB <sub>9</sub> H <sub>5</sub> Br <sub>5</sub> <sup>-</sup>		2.44	2.24	0.46	13
Me	pyridine	I <sup>-</sup>	1.86	1.73	0.61	24
Ph	OCIO <sub>3</sub> <sup>-</sup>		1.74	1.64	0.68	23
iPr	acetonitrile	<i>closo</i> -CB <sub>9</sub> H <sub>5</sub> Br <sub>5</sub> <sup>-</sup>	1.82	1.73	0.71	13

<sup>a</sup> Reference 22.

CB<sub>11</sub>H<sub>6</sub>Br<sub>6</sub><sup>-</sup>) through a bromine. In the first case the Si-N distance of 1.82 Å is only 0.1 Å longer than the normal Si-N value, and in the second and third cases the Si-Br distances are 0.20–0.24 Å longer than the normal (but larger) Si-Br value. The first elongation is comparable to those observed with Si-O in the structure of triphenylsilyl perchlorate<sup>23</sup> and with Si-N in the structure of SiMe<sub>3</sub> bound to pyridine,<sup>24</sup> and the others are slightly less than for Si-C in the present case.

These bond elongations may be transformed into bond orders by the equation derived by Pauling, eq 4,<sup>25</sup> in which

$$D(n) = D(1) - 0.60 \log n \quad (4)$$

$D(1)$  is the bond length for a normal bond of order 1.0 and  $D(n)$  is the bond length for a bond of order  $n$ . Traditionally, the value for  $D(1)$  has been taken to be the sum of the covalent radii, or 1.88 Å for C-Si. This value is actually outside the normal range mentioned above.<sup>22</sup> Use of 1.88 Å for  $D(1)$  would lead to the unsatisfactory result that a system with a normal length of, e.g., 1.84 Å has a bond order of 1.16. Thus we use 1.845 Å for  $D(1)$  in our calculations. The equation was solved for  $n$  for the set of compounds of interest in the present context, and these results are set out in Table 6.

The bond order of about 0.28 between silicon and the para carbon of toluene in the present study is the lowest by far and indicates that there is little covalent bonding between silicon and toluene. The complexes between triisopropylsilylium and carborane anions with bond orders of 0.40–0.46 described by Reed also have high silyl cation character or could be termed ion pairs.<sup>13</sup> The structures with acetonitrile,<sup>13</sup> pyridine,<sup>24</sup> and perchlorate<sup>23</sup> are predominantly covalent but still have significant ionic character, which results in a bond elongation of only about 0.1 Å. It is worth noting that the C-Si distance would have to be 2.45 Å for a bond order of 0.1.

Although the Pauling method is approximate and has been supplanted by more sophisticated calculational procedures, the bond orders in Table 6 have qualitative and relative validity. Schleyer et al.<sup>26</sup> calculated a Wiberg bond index of 0.44 for the complex between SiH<sub>3</sub><sup>+</sup> and benzene at the HF/6-31G\* level. As the SiH<sub>3</sub> group is much less able to sustain positive charge than SiEt<sub>3</sub>, the bond order for SiEt<sub>3</sub> should be less than 0.44, possibly much less, particularly as the calculations did not reproduce the structure well (*vide infra*). Thus modern theory confirms the Pauling approach and indicates that there

is only about one-third of a covalent bond between Si and the aromatic ring. It is of course possible that the bond order in condensed phase would differ from that in the gas phase. If anything, solvation should stabilize the charge of Et<sub>3</sub>Si<sup>+</sup> and reduce the bond order. These Pauling and Wiberg bond orders are clearly lower than those in any other structurally determined Si-X system.

The low bond order in the crystal is consistent with the behavior of trialkylsilylium in aromatic solvents. The low degree of covalent bonding is indicated by the rapid exchange between the silicon and arenes on the NMR time scale (the single <sup>29</sup>Si peak observed in mixed arene solvents; homotopic isopropyl methyl peaks in methylidisopropylsilylium). Moreover, Reed et al.<sup>13</sup> recrystallized silylium salts very similar to ours from arene solvents without reaction. The poor ability of trialkylsilyl chlorides to silylate arenes under Friedel-Crafts conditions is consistent with these observations.

Despite the long distance of the C-Si interaction, the geometry around silicon is clearly pyramidal. The Si atom is about 0.45 Å out of the plane of the three attached carbon atoms. This value is comparable to those of the other cases listed in Table 6, with the exception of the second entry. It is clear that this molecule, prepared by Reed et al.,<sup>13</sup> is the closest approach geometrically to a tricoordinate silyl cation. Pyramidalicity, however, is remarkably insensitive to the distance to the fourth coordination.

An alternative approach to characterizing these species is to assess the proportions of positive charge on silicon and on the fourth ligand. A silylium ion must have the preponderance of charge on silicon. Schleyer and co-workers have carried out *ab initio* calculations that place +0.71 on Si in Me<sub>3</sub>Si(toluene)<sup>+</sup>, a model for the present molecule, whereas they calculate only +0.43 on Si of Me<sub>3</sub>-SiH.<sup>26</sup> Thus theory confirms that most of the charge is on silicon and only a fraction of the charge is left to be distributed over the atoms of toluene. The structural deficiencies of the calculation (*vide infra*) suggest that there would be an even larger actual positive charge on Si for a molecule whose geometry corresponds more precisely to that of the observed structure.

Additionally, there are several experimental approaches to determining the location of the positive charge. If the positive charge is on the carbons of the toluene, the ion would be termed arenium (a  $\sigma$  or Wheland complex). The arenium ion model for the present molecule would resemble 1. The crystal structures for several arenium ions have been reported (none with silicon). The aromatic rings in these known  $\sigma$  complexes variously have several methyl or pyrrolidino groups (X, Y in 2) on the five sp<sup>2</sup> carbons (1, 2, 2', 3, 3' in 2) to stabilize the positive charge. These substituents ensure that positive charge is brought to the aromatic ring from the R, R' substituents, so that 2 provides the best model for a true  $\sigma$  complex (arenium ion). The sixth carbon (4), which is sp<sup>3</sup> hybridized, has substitution

(23) Surya Prakash, G. K.; Keyaniyan, S.; Aniszfeld, R.; Heiliger, L.; Olah, G. A.; Stevens, R. C.; Choi, H.-K.; Bau, R. *J. Am. Chem. Soc.* 1987, 109, 5123–5126.

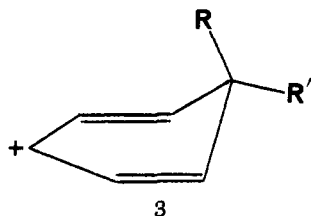
(24) Hensen, K.; Zengerly, T.; Pickel, P.; Klebe, G. *Angew. Chem., Int. Ed. Engl.* 1983, 22, 725–727.

(25) Pauling, L. *The Nature of the Chemical Bond*, 3rd ed.; Cornell University Press: Ithaca, NY, 1960; p 255. Pauling, L. *Science* 1994, 263, 983.

(26) Schleyer, P. v. R.; Buzek, P.; Müller, T.; Apeloig, Y.; Siehl, H.-U. *Angew. Chem., Int. Ed. Engl.* 1993, 32, 1471–1473.



patterns (R, R') that include CH<sub>2</sub>, CHCH<sub>3</sub>, C(CH<sub>3</sub>)<sub>2</sub>, C(CH<sub>3</sub>)(C<sub>6</sub>H<sub>5</sub>), or CHBr. The geometries, despite these structural variations, have a number of common structural characteristics that distinguish them from the present structure. (1) In the arenium ions, C4 is clearly sp<sup>3</sup>, with bond angles (both inside and outside the ring) in the range 107–115°. (2) There is severe bond alternation, with a short 23 bond and long 12 and 34 bonds, indicative of a quinoidal structure. The 34/23/12 bond lengths are 1.505/1.375/1.414, 1.50/1.38/1.425, 1.515/1.385/1.425, 1.49/1.365/1.405, and 1.50/1.37/1.415 Å for the systems reported by Effenberger et al.<sup>27</sup> (3) C4 deviates considerably from the plane of the other five atoms (3). This distortion is best

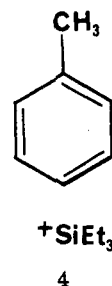


illustrated by the dihedral angles within the ring, which would be 0° for a planar geometry. For an unsymmetrically substituted case (R ≠ R') as in 1, the 2343' dihedral angle is 18.5°, the 1234 dihedral angle is 6.9°, and the 1'123 angle is 6.5°.<sup>27</sup> (4) The bonds to R and R' are relatively normal, 1.56 Å to CH<sub>3</sub> and 1.58 Å to C<sub>6</sub>H<sub>5</sub>, compared with the normal 1.54 Å.

The coordinated toluene molecule in the present structure contrasts appreciably with these structures. (1) C4 is close to sp<sup>2</sup>: ∠343' is 118° and ∠34H is 121°. (2) There is little bond alternation: 1.40, 1.37, and 1.38 Å for 34, 23, and 12. (3) The ring is very close to planarity, the dihedral angles being 0 (2'123), 1.5 (1234), and 2.8° (2343'). (4) As already mentioned, the C–Si distance of 2.18 Å is much larger than the normal distance of 1.85 Å. These geometrical characteristics indicate a very modest amount of perturbation (slight deviations of C4 from sp<sup>2</sup>, small bond alternation) of the toluene by the triethylsilyl group, suggesting very little arenium ion character of the present ion. Schleyer et al.<sup>26</sup> cited as an analogy an arenium ion that is planar and lacks bond alternation but which is symmetrical and spiroconjugated. The spiroconjugative interaction, however, is optimized by planarity and bond equality in the arenium portion, so that the model is entirely inappropriate in the present context.

The presence of silicon alters the nature of the structure. By analogy with the β effect,<sup>28</sup> whereby silicon stabilizes positive charge at a β position (Si–C–C<sup>+</sup>), silicon can stabilize charge on a cyclohexadienyl cation. Hyperconjugation in fact removes charge from the ring and places

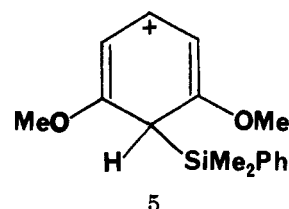
it on silicon, as in 4. Thus, to the extent that hypercon-



jugation is present, the σ complex or arenium ion is replaced by a silyl cation and an unperturbed arene ring. Therefore invoking hyperconjugation favors a silyl cation model for the present structure.

Simple, saturated β-effect cations have never been isolated, as the silyl group is easily expelled.<sup>29</sup> One isolated β-silyl ion (a β-silylallyl ion) in fact had the C–Si bond arranged orthogonally to the empty p orbital, so that there could be no direct electronic interaction,<sup>29</sup> and the species therefore was not a β-effect cation. Some β-silylvinyl cations have also been observed.<sup>30</sup>

Lew and McClelland,<sup>31</sup> using laser flash photolysis, recently reported direct observation of cation 5, as a short-



lived species in hexafluoro-2-propanol. They found rate constants for expulsion of R<sub>3</sub>Si of 10<sup>4</sup>–10<sup>5</sup> s<sup>-1</sup>, depending on the R group, figures that confirm the previous difficulties in isolating β-effect cations. The stability of our material contrasts with their observations. Without structural data on 5, it is not clear how similar it is to the molecule whose X-ray structure we report.

It is noteworthy that the calculations of Schleyer et al.<sup>26</sup> do not accurately reproduce the observed geometry of our X-ray structure, even though they accurately calculate the <sup>29</sup>Si chemical shift. First, they calculate strong alternation within the toluene ring of 1.405/1.367/1.429 Å, whereas the observed result is 1.38/1.37/1.40 Å. Second, the Si–C distance (from C4 to Si) is calculated to be 2.14 Å but observed to be 2.18 Å. Finally, and most critically, the angle between the Si–C4 bond and the C4–C1 vector is calculated to be 114° but observed to be 104°. Although experimental error in the X-ray structure can explain these deviations in part, nonetheless in each quantity the calculations portray a species with higher arenium ion character and hence lower silylium ion character than is observed for the actual molecule in the crystal. The calculations of course refer to the gas phase, and the differences between calculated and observed structures may be attributed to the differences in phase. The gas-

(27) Effenberger, F.; Reisinger, F.; Schönwälder, K. H.; Bäuerle, P.; Stezowski, J. J.; Jogun, K. H.; Schöllkopf, K.; Stohrer, W.-D. *J. Am. Chem. Soc.* **1987**, *109*, 882–892.

(28) Lambert, J. B. *Tetrahedron* **1990**, *45*, 2677–2689.

(29) Olah, G. A.; Berrier, A. L.; Field, L. D.; Surya Prakash, G. K. *J. Am. Chem. Soc.* **1982**, *104*, 1349–1355. Surya Prakash, G. K.; Reddy, V. P.; Rasul, G.; Casanova, J.; Olah, G. A. *J. Am. Chem. Soc.* **1992**, *114*, 3076–3078.

(30) Siehl, H.-U.; Kaufmann, F.-P. *J. Am. Chem. Soc.* **1992**, *114*, 4937–4939.

(31) Lew, C. S. Q.; McClelland, R. A. *J. Am. Chem. Soc.* **1993**, *115*, 11516–11520.

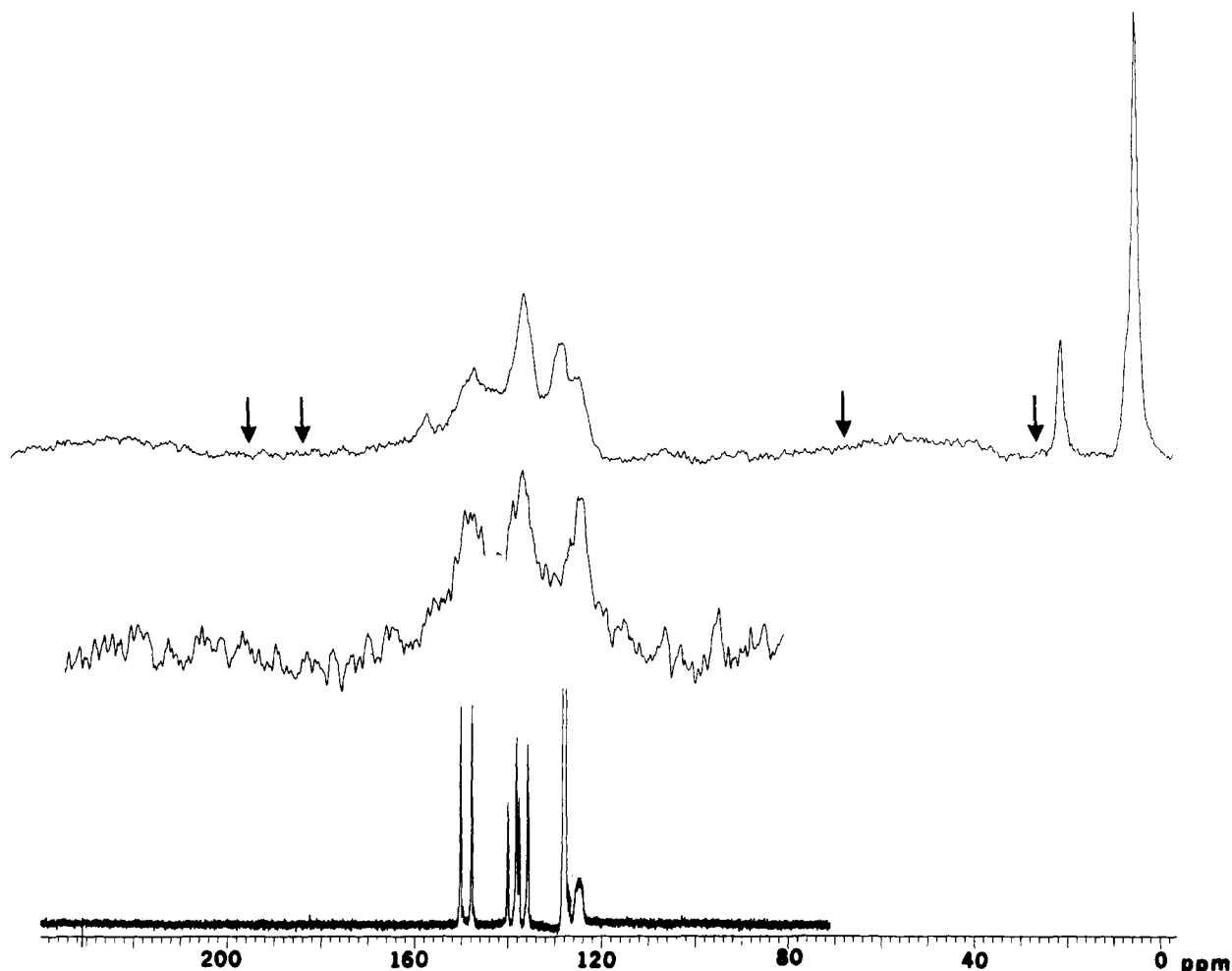


**Figure 7.** Top: Solid-state (CP/MAS)  $^{13}\text{C}$  spectrum of  $[\text{Et}_3\text{Si}][\text{TPFPB}]\cdot 2\text{toluene}$ . Middle: Solid-state (CP/MAS)  $^{13}\text{C}$  spectrum of lithium tetrakis(pentafluorophenyl)borate etherate. Bottom:  $^{13}\text{C}$  spectrum of lithium tetrakis(pentafluorophenyl)borate etherate in benzene (the sharp peak at  $\delta$  128 is from the solvent). Spectra were recorded at a frequency of 75 MHz.

phase molecule would tend to be tighter and hence have higher arenium character.

The  $^{13}\text{C}$  spectrum of the arene portion of our structure also should characterize the extent of positive charge that resides in the arene ring. The chemical shifts of the aromatic carbons of free toluene are at  $\delta$  137.8 (i), 129.3 (o), 128.5 (m), and 125.6 (p), and that of the methyl carbon is at  $\delta$  21.3.<sup>32</sup> Although protonated toluene has not been studied, the  $^{13}\text{C}$  chemical shifts of protonated mesitylene are known.<sup>33</sup> The methyl-substituted carbon moves from  $\delta$  137.6 to 194.2, the protonated carbon moves from  $\delta$  127.4 to 54.5, the unprotonated and unmethylated carbon moves from  $\delta$  127.4 to 135.4, and the methyl moves from  $\delta$  21.2 to 27.5. Thus the  $^{13}\text{C}$  chemical shifts are strongly influenced by the presence of positive charge. We cannot measure the chemical shifts for the liquid, because the ligand toluene exchanges rapidly. In toluene or another aromatic solvent, the observed chemical shifts would be weighted averages with the preponderance of uncoordinated solvent. Thus we measured the shift in the solid, with CP/MAS techniques. This procedure also ensured that we were examining exactly the same species to which the X-ray structure corresponds. In order to examine the toluene complex of triethylsilylium tetrakis(pentafluoro-

rophenyl)borate, we dissolved the solvent-free salt in toluene and added hexane to reprecipitate the solid, now reconstituted with toluene. This solid was examined by  $^{29}\text{Si}$  and  $^{13}\text{C}$  NMR spectroscopies.

The expected positions for the toluene complex may be calculated from those of the mesitylene complex from the known effects of the different substituent patterns in (trimethylsilyl)benzene and protonated mesitylene. The expected chemical shifts for a toluenium ion are  $\delta$  194.4 (i), 137.3 (o), 185.1 (m), 69.2 (p), and 27.6 ( $\text{CH}_3$ ) (i, o, m, and p are with respect to the methyl-substituted position).

Figure 7 (top) depicts the CP/MAS spectrum for triethylsilylium tetrakis(pentafluorophenyl)borate precipitated from toluene and hexane. The furthest upfield peak at  $\delta$  5.0 is from the carbons of the ethyl groups. The next singlet, at  $\delta$  21.0, is from the methyl group of toluene. The arrow adjacent to it indicates where the methyl group would fall for the toluenium ion ( $\delta$  27.6). It is clear that the methyl resonance corresponds to that of free toluene. As each unit cell contains two coordinated and two free toluene molecules, they are indistinguishable by  $^{13}\text{C}$  NMR spectroscopy (only one methyl resonance).

The aromatic region contains resonances both from toluene and from the anion. As a model for the anion, we recorded spectra of lithium tetrakis(pentafluorophenyl)borate etherate in the solid (Figure 7, middle) and in benzene (bottom). The solution peaks show the expected

(32) Stothers, J. B. *Carbon-13 NMR Spectroscopy*; Academic Press: New York, 1972; pp 97, 98.

(33) Koptug, V.; Rezvukhin, A.; Lippmaa, E.; Pehk, T. *Tetrahedron Lett.* 1968, 4009-4012.

splitting by  $^{19}\text{F}$ . In the solid, the resonances have almost the same groupings, around  $\delta$  147 (m), 136 (o, p), and 123 (i). In this system cross polarization (CP) produces no benefit, as there are no protons on the aromatic rings. Thus the ipso resonance becomes as large as the para resonance. The superposition of the toluene resonances (with CP) on top of the anion resonances (Figure 7, top) shows a new peak at  $\delta$  128 (ortho and meta carbons of free toluene) and enhanced intensity at  $\delta$  137 (ipso carbon of free toluene). The para carbon of free toluene would fall on top of the  $\delta$  125 peak. Thus all of the new peaks, superimposed on top of those of the anion, correspond to the positions of free toluene. The arrows indicate the expected positions for the toluenium ion, with the carbons ipso and meta to methyl (ortho and para to  $\text{Et}_3\text{Si}$ ) displaced to low field by the presence of positive charge and the carbon para to methyl (ipso to  $\text{Et}_3\text{Si}$ ) displaced to high field by rehybridization to  $\text{sp}^3$ . There are no peaks remotely close to these positions. The small peak at  $\delta$  157 may be a spinning sideband, as it moved (and other peaks did not) when the experiment was repeated on a new sample. At the end of this experiment, which required 24–72 h on the spectrometer, we retook the  $^{29}\text{Si}$  spectrum to confirm that the sample was still the silyl cation and not a decomposed material. The primary peak was indeed at  $\delta$  92.8, although smaller peaks ( $\delta$  37, 56) indicated that minor decomposition had occurred. The spectrum clearly rejects a classical  $\sigma$  complex or arenium ion model, for which positive charge resides on the arene ring. It is consistent with charge primarily on silicon, as in the silylium model (4).

As suggested by Reed, C–Si hyperconjugation, only possible if there is a substantial concentration of positive charge on silicon, may play a major role in determining the geometry of the cation in the crystal. As seen in Figures 3 and 4, the C4–C5 or C18–C19 bond is well-positioned for  $\text{C}^+ \text{C}=\text{Si}$  hyperconjugation in one ethyl arm. The hydrogen atoms are less well defined, but hydrogens on C2 and C6 (Figure 3) or C16 and C20 (Figure 4) are well positioned for  $\text{H}^+ \text{C}=\text{Si}$  hyperconjugation in the other two ethyl arms. The particular arrangement of the three ethyl groups is otherwise determined by steric interactions with one another and with the toluene molecule.

### Conclusions

The first piece of evidence that ions formed by eq 1 with X as  $(\text{C}_6\text{F}_5)_4\text{B}^-$  (TPFPB) and arenes as solvents have high silyl cation character is the low-field  $^{29}\text{Si}$  chemical shifts reported in Table 1. For alkyl substituents these shifts are some 50 ppm downfield from those of the corresponding perchlorates and show a gradation when the arenes are replaced by solvents with increasing nucleophilicity. In the case of the substituent  $\text{Me}_3\text{Si}$  on silicon (R in eq 1), the total shift from the corresponding silane is 228.5 ppm. We believe that this species most closely resembles the expectations for a pure silyl cation, but we cannot say how close to the ideal it is. It is clear from the NMR spectra that there is little or no interaction between the cation and the borate anion in solution. This may not be the case in the solid. The  $^{29}\text{Si}$  chemical shifts of these species in the solid, having been generated in the absence of any solvent other than the starting silane, are very similar to those in the arene solvents, indicating that the anion or some other entity must serve a coordinating role in the solid similar to that of the arene solvents in solution.

The complexes between silyl cation and solvent exist as dynamic structures. The isopropyl methyl groups of the substituents in the system  $\text{MeiPr}_2\text{SiH}$  are diastereotopic and nonequivalent in the  $^1\text{H}$  and  $^{13}\text{C}$  spectra but become equivalent on conversion to the TFPB salt in all solvents. This observation suggests a barrier to interconversion, which must include breaking the bonding interaction between Si and solvent, of no more than about 13 kcal  $\text{mol}^{-1}$ , which corresponds to the NMR time scale for the temperature and chemical shift differences involved. The interaction between silicon and solvent thus is a severely weakened covalent bond.

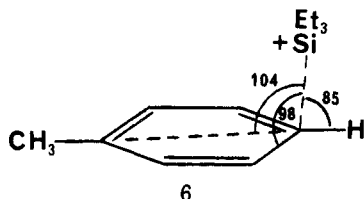
The crystal structure of triethylsilylium tetrakis(pentafluorophenyl)borate recrystallized from mixtures of toluene and hexane agrees with the overall conclusions based on the spectra recorded in arene solution. There is no interaction between the anion and the cation, as the closest approach between Si and F is more than 4 Å. The solvent toluene resides in a fourth coordination position but is at a greater distance than ever observed previously for a covalent C–Si bond. The distance (2.18 Å) corresponds to a C–Si bond order of about 0.28 according to the Pauling equation. The toluene molecule shows little perturbation in geometry from that of free toluene. These observations indicate that silicon is strongly positively charged and little charge is transferred to the carbons on toluene. Full bonding to carbon and complete transfer of charge would result in a description of the species as an arenium ion (1), but the observed geometry does not correspond to such a toluenium ion. Such species have been well characterized in the literature by electronic and NMR spectroscopies. For our species the CP/MAS  $^{13}\text{C}$  chemical shifts of the coordinated toluene are unperturbed from those of free toluene, so that the arenium structure is entirely inappropriate.

Reed et al.<sup>13</sup> also have rejected the arenium ion model and have suggested that the bonding between  $\text{Et}_3\text{Si}^+$  and toluene is an  $\eta^1 \pi$  complex. They had previously observed a benzene complex with  $\text{Ag}^+$  having bonding of this type.<sup>34</sup> Eaborn noted that a complex between  $\text{Li}^+$  and a phenyl group also is a strong structural analogy.<sup>35</sup> The key structural distinction between a  $\pi$  and a  $\sigma$  complex is that the former retains  $\text{sp}^2$  hybridization at the point of binding, whereas the latter has a rehybridized  $\text{sp}^3$  carbon to which Si is attached. The idealized angle between the Si–C4 vector and the C4–C1 vector (see 2) is  $90^\circ$  for a  $\pi$  complex and  $124^\circ$  for a  $\sigma$  complex. For comparison, it is  $94^\circ$  in the  $\text{Ag}^+$  complex with benzene,  $101^\circ$  in the  $\text{Li}^+$  complex with phenyl,<sup>35</sup> and  $104^\circ$  for the complex of  $\text{Et}_3\text{Si}^+$  with toluene. The literature precedents have referred to these structures as  $\pi$ , not  $\sigma$ , complexes. The Si–C4–C3 angle at  $98.4(7)^\circ$  and the Si–C4–H angle at  $85(4)^\circ$  in the present structure confirm that silicon is nearly perpendicular to the aromatic ring in all dimensions, so that bonding primarily involves  $\pi$  rather than  $\sigma$  orbitals (6). We believe that this bonding model, in which the positive charge is largely concentrated on silicon, best describes our crystal structure.

The silicon structures discussed herein, including all those in Table 6, represent several points along the dissociation continuum,  $\text{Si-X} \leftrightarrow \text{Si}^+ \text{X}^-$  or  $\text{Si-N}^+ \leftrightarrow \text{Si}^+ \text{N}^-$ . The range of  $^{29}\text{Si}$  chemical shift differences ( $\Delta\delta$ ) in Table 1, the range of bond elongations in Table 6 (observed

(34) Shelly, K.; Finster, D. C.; See, Y. J.; Scheidt, W. R.; Reed, C. A. *J. Am. Chem. Soc.* 1985, 107, 5955–5959.

(35) Eaborn, C.; Hitchcock, P. B.; Smith, J. D.; Sullivan, A. C. *J. Chem. Soc., Chem. Commun.* 1983, 1390–1391.



lengths compared with the length for  $n = 1$ ), and the range of R-Si-R angles for these same systems indicate that there is a continuum of structures of which the current examples (here and ref 13) represent the highest degree of silyl cation character observed to date in a structurally defined system.

The  $^{29}\text{Si}$  chemical shift of alkyl- and aryl-substituted cases in solution and the solid, the homotopic isopropyl groups in  $\text{MeiPr}_2\text{SiTPFPB}$ , the  $^{13}\text{C}$  spectrum and almost unperturbed geometry of the coordinated toluene in the solid, and the long crystallographic distance between silicon and toluene give a comprehensive description of a cation in which positive charge is predominantly but not exclusively on silicon and in which the fourth coordination is weak. The silyl-substituted case,  $(\text{Me}_3\text{Si})_3\text{SiTPFPB}$ , from its  $^{29}\text{Si}$  chemical shift appears to be closest to the tricoordinate ideal.

### Experimental Section

**Methyldiisopropylsilane.** Into a three-necked flask were placed 10 g (54 mmol) of diisopropyldichlorosilane and 25 mL of tetrahydrofuran (THF). A 3 M solution of methylmagnesium bromide in 20 mL of THF (60 mmol) was added, and the mixture was stirred overnight. The volatile materials were removed by distillation at reduced pressure, leaving the magnesium salts behind. These volatiles comprised a solution of methyldiisopropylchlorosilane in THF. To this solution was added 2 g of  $\text{LiAlH}_4$ , and the mixture was stirred overnight. The volatiles again were removed from the salts by vacuum distillation, and fractional distillation gave 6 g of methyldiisopropylsilane in 80% purity (68% yield). Purification by preparative gas chromatography yielded a product of 97.3% purity. Anal. Calcd for  $\text{C}_7\text{H}_{18}\text{Si}$ : C, 64.52; H, 13.92. Found: C, 64.73; H, 13.93.

**Tris(pentafluorophenyl)borane.**<sup>36</sup> Into an oven-dried, 1000-mL, three-necked flask, equipped with a mechanical stirrer, a  $\text{N}_2$  inlet tube, and a rubber septum, was distilled 600 mL of pentane, which had previously been refluxed with  $\text{LiAlH}_4$  overnight. The flask was placed in a dry ice bath, and 18 g (0.073 mol) of pentafluorobromobenzene was added. The flask was placed behind a protective shield, and 28 mL of 2.5 M  $\text{BuLi}$  was added with the temperature of the solution maintained at  $-78^\circ\text{C}$ . The mixture was stirred for 15 min, and 2.3 g (0.02 mol) of  $\text{BCl}_3$  was added. The solution was stirred for an additional 15 min, the dry ice bath was removed, and the stirring was stopped. The reaction mixture was allowed to warm slowly to room temperature, and the clear top solution was removed by cannulation. The residue was removed and filtered off under  $\text{N}_2$ . The solvent was removed at reduced pressure, with all transfers carried out under  $\text{N}_2$ , to give 2.4 g (23.4%) of an off-white solid.

**Lithium Tetrakis(pentafluorophenyl)borate.**<sup>37</sup> Pentafluorophenyllithium (10 mmol) was prepared by the reaction of pentafluorobromobenzene (2 g, 8 mmol) in anhydrous ether with 3.2 mL of 2.5 M  $\text{BuLi}$  at  $-78^\circ\text{C}$ . This solution was added by cannulation to 4 g (7.8 mmol) of tris(pentafluorophenyl)borane dissolved in 100 mL of pentane, and the mixture was cooled to  $-78^\circ\text{C}$ . The solution was stirred for 15 min, and the cooling bath was removed. Stirring was continued at room temperature for

1 h. The product formed as a white precipitate, which was isolated by filtration. Solvent was further removed by exposure of the solid to vacuum overnight, to produce 3.17 g (59%) of lithium tetrakis(pentafluorophenyl)borate.

**Triphenylmethyl (Trityl) Tetrakis(pentafluorophenyl)borate.**<sup>14</sup> Lithium tetrakis(pentafluorophenyl)borate (3.17 g, 4.62 mmol) was placed in a 500-mL, three-necked flask. Trityl chloride (1.54 g, 5.54 mmol) suspended in 200 mL of hexane (dried over  $\text{LiAlH}_4$ ) was added to the flask, which was evacuated and filled with  $\text{N}_2$ . The mixture was stirred at room temperature for 1 h, as a yellow precipitate formed. The hexane was removed by syringe, and the solid was treated with 100 mL of  $\text{CH}_2\text{Cl}_2$ . The insoluble  $\text{LiCl}$  was removed by filtration, and the solution was concentrated under vacuum to about 30 mL. Upon addition of 30 mL of hexane, a yellow oil formed, which solidified with stirring. The solvent was decanted, and the yellow solid was dried under vacuum to give 2.6 g (61%) of the product.

**Triethylsilylium Tetrakis(pentafluorophenyl)borate.** Triethyl tetrakis(pentafluorophenyl)borate (200 mg) was placed in a 10 mm o.d. NMR tube, which was evacuated and placed under a  $\text{N}_2$  atmosphere. Triethylsilane (1 mL), which had been distilled over  $\text{LiAlH}_4$ , was added via syringe, the mixture was frozen, and the tube was evacuated and sealed. The yellow solid gradually was replaced with a white powder. After 2 days, the liquid was removed by cannulation, and the solid was washed with 1 mL of dry hexane to remove the triphenylmethane byproduct. The yield was virtually quantitative. This solid was examined directly by CP/MAS NMR. When the solid was mixed with  $\text{C}_6\text{D}_6$ , two layers formed. The top layer was a very dilute solution of the triethylsilylium borate, and the lower, oiled-out layer was almost pure silylium borate with some benzene. The lower layer was easily analyzed by  $^{29}\text{Si}$  NMR spectroscopy, as well as for other, more sensitive nuclides. The preparation also may be carried out from the beginning in a solvent such as  $\text{C}_6\text{D}_6$ . For X-ray analysis, the washed, white powder was taken up into a large quantity of dry toluene, about 10 mL/mg of silylium borate. Hexane was then added to bring about crystal formation. At 1/1 hexane/toluene, no crystals formed at room temperature but needles formed in the freezer. At a 2/1 ratio, crystals formed at room temperature.

**Other Silylium Tetrakis(pentafluorophenyl)borates.** The same procedure as for triethylsilylium was used in all other cases. Clean reactions were obtained for trimethylsilyl, triisopropylsilyl, triisobutylsilyl, trihexylsilyl, methyl-diphenylsilyl, and methyl-diisopropylsilyl, as indicated by a single set of peaks in the  $^1\text{H}$  and  $^{13}\text{C}$  spectra and by only one peak in the  $^{29}\text{Si}$  spectrum. For tris(trimethylsilyl)silane, the lowest field  $^{29}\text{Si}$  peak was accompanied by one or two other peaks of comparable or smaller intensity. Triphenylsilane, ethyldimethylsilane, dimethyl[(trimethylsilyl)methyl]silane, and diphenyl[(trimethylsilyl)methyl]silane appeared to react in the normal fashion, but examination of the NMR spectra indicated a variety of products, e.g., multiple  $^{29}\text{Si}$  peaks, at not lower field than  $\delta$  60. The reactions with *tert*-butylsilane and cyclohexyldi-*tert*-butylsilane were extremely sluggish and also gave mixtures. In these cases the products were not identified.

**NMR Spectra.** Solution NMR spectra were recorded on a Varian XLA-400 spectrometer, and solid-state NMR spectra were recorded on a Varian VXR-300 spectrometer. Solid-state  $^{29}\text{Si}$  spectra were referenced to external hexamethyldisiloxane and scaled to TMS. The spinning rate was 4000–6000 Hz, the pulse width was 4.8  $\mu\text{s}$ , the pulse delay was 15 s, and 4000–6000 transients were taken. Solid-state  $^{13}\text{C}$  spectra used a spinning rate of 2000–4000 Hz, a pulse width of 4.8  $\mu\text{s}$ , a delay time of 5 s, and 15 000–45 000 transients. For liquid-state  $^{29}\text{Si}$  spectra, the pulse width was 13.0  $\mu\text{s}$ , the pulse delay was 2.5 s, and the number of transients was 10 000–15 000.

**Product Analysis.** For the case of tris(trimethylsilyl)silane, the ionic solution was allowed to react with diisobutylaluminum hydride (dIBALH) in order to analyze the products. In a 10-mm NMR tube on the vacuum line, 300 mg (0.325 mmol) of trityl tetrakis(pentafluorophenyl)borate in 1 mL of toluene was allowed

(36) Massay, A. G.; Park, A. G. In *Organometallic Synthesis*; King, R. B., Kisch, J. J., Eds.; Elsevier: New York, 1986; Vol. 3, p 461.

(37) Massay, A. G.; Park, A. J. *J. Organomet. Chem.* 1964, 2, 245–250.

Table 7. Crystallographic Parameters

empirical formula	SiF <sub>20</sub> C <sub>44</sub> BH <sub>27</sub>
fw	974.56
crystal dimens	0.26 × 0.48 × 0.14 mm <sup>3</sup>
crystal system	triclinic
ω-scan peak width at half-height	0.30
lattice params	<i>a</i> = 13.168(4) Å <i>b</i> = 17.593(3) Å <i>c</i> = 18.177(4) Å α = 86.19(2)° β = 84.21(2)° γ = 82.24(2)° <i>V</i> = 4131(3) Å <sup>3</sup>
space group	<i>P</i> $\bar{1}$ (No. 2)
<i>Z</i> value	4
<i>D</i> <sub>calc</sub>	1.567 g cm <sup>-3</sup>
<i>F</i> <sub>000</sub>	1960
μ(Mo Kα)	1.74 cm <sup>-1</sup>
radiation	Mo Kα (λ = 0.710 69 Å)
attenuator	Zr foil (factor = 22.3)
takeoff angle	2.8°
detector aperture	2.0–2.5 mm horizontal 2.0 mm vertical
crystal to detector dist	21 cm
scan rate	3.0–16.0° min <sup>-1</sup> (in ω)
anomalous dispersion	all non-hydrogen atoms
no. of observns ( <i>I</i> > 3.00σ( <i>I</i> ))	4627
no. of variables	751
refln/param ratio	6.16
residuals: <i>R</i> , <i>R</i> <sub>w</sub>	0.069, 0.066
goodness of fit indicator	1.93
max shift/error in final cycle	0.15

to react with 80 mg (0.325 mmol) of tris(trimethylsilyl)silane at -20 °C. The reaction mixture was kept at this temperature overnight, and a syringed sample was found by GC to contain no starting silane. diBALH (0.1 mL) was added slowly to the mixture, and a single phase was obtained after 1 h. Degassed H<sub>2</sub>O was added slowly, and the solution bubbled vigorously. The organic layer was analyzed by GC and GCMS, and the predominant product was found to be tris(trimethylsilyl)silane, the regenerated starting material. By comparison with Ph<sub>3</sub>CH as an internal standard, the yield was >25%.

**Crystallographic Analysis.** A colorless, prismatic crystal with approximate dimensions 0.26 × 0.48 × 0.14 mm was mounted on a glass fiber. All measurements were carried out on an Enraf-Nonius CAD-4 diffractometer with graphite-monochromated Mo Kα radiation. Cell constants and an orientation matrix for data collection, obtained from a least-squares refinement with the setting angles of 25 carefully centered reflections in the range 18.2 < 2θ < 26.0°, corresponded to a triclinic cell with dimensions given in Table 7. For *Z* = 4 and fw 974.56 (which includes two molecules of toluene per silylium borate unit), the calculated density was 1.567 g cm<sup>-3</sup>. On the basis of packing considerations and a statistical analysis of intensity distribution, the space group was determined to be *P* $\bar{1}$ . The data were collected at -120 ± 1 °C with the ω-θ scan technique to a maximum 2θ of 48.0°. ω scans of several intense reflections, made prior to data collection, had an average width at half-height of 0.30° with a takeoff angle of 2.8°. Scans of (1.00 + 0.35 tan θ) were made at speeds ranging from 3.0 to 16.0 min<sup>-1</sup> in ω. Moving-crystal, moving-counter background measurements were made by scanning an additional 25% above and below the scan range. The counter aperture consisted of a variable horizontal slit set to 2.0 mm. The diameter of the incident beam collimator was 0.7 mm, and the distance

from crystal to detector was 21 cm. For intense reflections, an attenuator was automatically inserted in front of the detector. Of the 13 573 reflections that were collected, 12 933 were unique (*R*<sub>int</sub> = 0.070). The intensities of three representative reflections measured every 90 min during X-ray exposure remained constant throughout data collection, indicating crystal and electronic stability. No decay correction was applied. The linear absorption coefficient for Mo Kα is 1.7 cm<sup>-1</sup>. An analytical absorption correction was applied, which resulted in transmission factors ranging from 0.95 to 0.98. The data were corrected for Lorentz and polarization effects. The structure was solved by direct methods in the space group *P*1 and then converted to the actual space group of *P* $\bar{1}$ .<sup>38</sup> Because of the large number of atoms in the unit cell compared with the amount of available data, only silicon and fluorine atoms were refined with anisotropic thermal coefficients. Except for H53 and H54 (the para hydrogens in the coordinated toluenes), all hydrogen atoms were included as fixed contributors at idealized positions with the thermal parameter set to 1.2 times the carbon thermal parameter. The final cycle of full-matrix, least-squares refinement was based on 4627 observed reflections (*I* > 3.00σ(*I*)) and 751 variable parameters. The function that was maximized was Σw(|*F*<sub>o</sub>| - |*F*<sub>c</sub>|)<sup>2</sup>, in which *w* is 4*F*<sub>o</sub><sup>2</sup>/σ<sup>2</sup>(*F*<sub>o</sub><sup>2</sup>), σ<sup>2</sup>(*F*<sub>o</sub><sup>2</sup>) is [S<sup>2</sup>(*C* + *R*<sup>2</sup>*B*) + (*pF*<sub>o</sub><sup>2</sup>)<sup>2</sup>]/(*Lp*)<sup>2</sup>, *S* is the scan rate, *C* is the total integrated peak count, *R* is the ratio of scan time to background counting time, *B* is the total background count, *Lp* is the Lorentz-polarization factor, and *p* is the *p* factor. At convergence, the largest parameter shift was 0.15 times its esd, the unweighted agreement factor *R* = Σ||*F*<sub>o</sub>| - |*F*<sub>c</sub>||/Σ|*F*<sub>o</sub>| was 0.069, and the weighted agreement factor *R*<sub>w</sub> = [Σw(|*F*<sub>o</sub>| - |*F*<sub>c</sub>||)<sup>2</sup>/Σw*F*<sub>o</sub><sup>2</sup>]<sup>1/2</sup> was 0.066. The standard deviation of an observation of unit, [Σw(|*F*<sub>o</sub>| - |*F*<sub>c</sub>||)<sup>2</sup>]/(*N*<sub>o</sub> - *N*<sub>v</sub>)<sup>1/2</sup>, in which *N*<sub>o</sub> is the number of observations and *N*<sub>v</sub> is the number of variables, was 1.93. The weighting scheme was based on counting statistics and included a factor *p* = 0.03 to downweight intense reflections. The maximum and minimum peaks on the final difference Fourier map corresponded to 0.62 and -0.40 electron Å<sup>-3</sup>, respectively. Neutral-atom scattering factors were taken from Cromer and Waber.<sup>39</sup> Anomalous dispersion effects were included in *F*<sub>c</sub> for all non-hydrogen atoms.<sup>40</sup> The values of *f*' and *f*'' were those of Cromer.<sup>41</sup> All calculations were performed with the TEXSAN crystallographic software package of the Molecular Structure Corp. (1985).

**Acknowledgment.** This work was supported by the National Science Foundation (Grant No. CHE-9302747) and the donors of the Petroleum Research Fund, administered by the American Chemical Society. The authors are indebted to Charlotte C. Stern (Northwestern University) and Dr. John C. Huffman (Indiana University) for carrying out the X-ray analysis.

**Supplementary Material Available:** Figures showing <sup>29</sup>Si spectra and a listing of thermal parameters (15 pages). Ordering information is given on any current masthead page.

OM9400715

(38) Sheldrick, G. M. SHELXS86. Program for the solution of crystal structures. University of Göttingen, Germany, 1986.

(39) Cromer, D. T.; Waber, J. T. *International Tables for X-ray Crystallography*; The Kynoch Press: Birmingham, U.K., 1974; Vol. IV, Table 2.2A.

(40) Ibers, J. A.; Hamilton, W. C. *Acta Crystallogr.* 1964, 17, 781-782.

(41) Cromer, D. T. *International Tables for X-ray Crystallography*; The Kynoch Press: Birmingham, U.K., 1974; Vol. IV, Table 2.3.1.